



A methods assessment and recommendations for improving calculations and reducing uncertainties in the determination of ^{210}Po and ^{210}Pb activities in seawater

Sylvain Rigaud, V. Puigcorbé, P. Cámara-Mor, N. Casacuberta, M. Roca-Martí, J. Garcia-Orellana, C. Benitez-Nelson, P. Masque, T. Church

► To cite this version:

Sylvain Rigaud, V. Puigcorbé, P. Cámara-Mor, N. Casacuberta, M. Roca-Martí, et al.. A methods assessment and recommendations for improving calculations and reducing uncertainties in the determination of ^{210}Po and ^{210}Pb activities in seawater. *Limnology and Oceanography: Methods*, 2013, 11 (10), pp.561-571. 10.4319/lom.2013.11.561 . hal-01717794

HAL Id: hal-01717794

<https://hal.science/hal-01717794>

Submitted on 27 Feb 2018

HAL is a multi-disciplinary open access archive for the deposit and dissemination of scientific research documents, whether they are published or not. The documents may come from teaching and research institutions in France or abroad, or from public or private research centers.

L'archive ouverte pluridisciplinaire **HAL**, est destinée au dépôt et à la diffusion de documents scientifiques de niveau recherche, publiés ou non, émanant des établissements d'enseignement et de recherche français ou étrangers, des laboratoires publics ou privés.

**A methods assessment and recommendations for improving calculations and reducing uncertainties
in the determination of ^{210}Po and ^{210}Pb activities in seawater**

Rigaud¹, S., Puigcorb  ^{2,3}, V., C  mara-Mor^{2,3}, P., Casacuberta^{2,3}, N., Roca-Mart  ^{2,3}, M., Garcia-Orellana^{2,3},
J., Benitez-Nelson⁴, C.R., Masqu  ^{2,3}, P., and Church^{1*}, T.

¹School of Marine Science and Policy, University of Delaware, Newark, Delaware 19716 USA.

²Departament de F  sica, Universitat Aut  noma de Barcelona, Barcelona 08193 Spain.

³Institut de Ci  ncia i Tecnologia Ambientals, Universitat Aut  noma de Barcelona, Barcelona 08193 Spain.

⁴Marine Science Program and Department of Earth and Ocean Sciences, University of South Carolina,
South Carolina 29208 USA.

Running Head: ^{210}Po and ^{210}Pb activity calculations in seawater

*Corresponding author

tchurch@udel.edu

Phone: (302) 831-2558

Fax: (302) 831-4575

19 **Acknowledgements**

20 The National Science Foundation grants (OCE-0851462) contributed to the manuscript and (OCE -
21 0961653) provided support for S. Rigaud. V. Puigcorbé, P. Cámara-Mor and M. Roca-Martí acknowledge
22 funding through PhD grants from the Ministerio de Educación y Ciencia (Spain). Funding was also
23 obtained through the ICREA Academia prize of the Generalitat de Catalunya and MEC CTM2007-31241-
24 E/MAR (P. Masque) and EU FP7-MC-IIF-220485 (C.R. Benitez-Nelson and P. Masqué). S. Rigaud also
25 wishes to thank Rachel Shelley for her initial assistance in writing the paper.

26

27

Abstract

In marine systems, ^{210}Po and ^{210}Pb disequilibria are being increasingly used to examine oceanic particle formation and export. Here, an updated assessment of current methods for determining ^{210}Po and ^{210}Pb activity in marine samples is provided and includes a complete description of the vast number of calculations and uncertainties associated with Po and Pb loss, decay, and ingrowth during sample processing. First we summarize the current methods for the determination of ^{210}Po and ^{210}Pb activities in dissolved and particulate seawater samples and recommend areas for improvement. Next, we detail the calculations and associated uncertainties using principles of error propagation, while also accounting for radionuclide ingrowth, decay and recovery. A spread-sheet reporting these calculations is included as a downloadable Web Appendix. Our analysis provides insight into the contributions of the relative uncertainty for each parameter considered in the calculation of final ^{210}Po and ^{210}Pb activities and gives recommendations on how to obtain the most precise final values. For typical experimental conditions in open seawater, we show that our method allows calculating ^{210}Pb activity with a relative uncertainty of about 7%. However for ^{210}Po activities, the final relative uncertainty is more variable and depends on the $^{210}\text{Po}/^{210}\text{Pb}$ activity ratio in the initial sample and the time elapsed between sampling and sample processing. The lowest relative uncertainties on ^{210}Po that can be obtained by this method is 6% and can only be obtained for samples with high $^{210}\text{Po}/^{210}\text{Pb}$ activity ratios (>1) that were rapidly processed.

Introduction

The naturally occurring ^{210}Po ($T_{1/2} = 138.4$ d) and ^{210}Pb ($T_{1/2} = 22.3$ y) radionuclide pair has been widely used to examine dissolved and particle dynamics in marine eco-systems over the past several decades (Bacon *et al.* 1976; Nozaki *et al.* 1976; Thomson and Turekian 1976; Masqué *et al.* 2002; Cochran and Masqué 2003; Rutgers van der Loeff and Geibert 2007). Both nuclides are part of the ^{238}U decay chain, with ^{210}Po produced from the decay of ^{210}Pb via ^{210}Bi ($T_{1/2} = 5.0$ d). In seawater, both ^{210}Pb and ^{210}Po are particle reactive, but ^{210}Po also bio-accumulates within organic tissues (Stewart and Fisher 2003a, 2003b; Stewart *et al.* 2005). As such, differences in the specific activity of these two radionuclides in the water column have been increasingly used to quantitatively assess export fluxes of sinking particulate material, such as organic carbon, from the surface ocean to depth (Moore and Dymond 1988; Sarin *et al.* 1999; Friedrich and Rutgers van der Loeff 2002; Stewart *et al.* 2007; Verdeny *et al.* 2009; Yang *et al.* 2011).

Since the fundamental measurement techniques described by Fleer and Bacon (1984), there have been significant improvements in sample processing that rely on the use of exchange resins (Sarin *et al.* 1992, Vajda *et al.*, 1994). While these methods have proven to be very successful in the separation of Po and Pb, losses of ^{210}Pb can occur during processing. Unfortunately, there is no clear consensus as to how such losses should be assessed during subsequent calculations. Some laboratories consider the loss as minor and ignore it, while others include extensive correction procedures. In addition, each laboratory has their own approach for calculating radionuclide ingrowth, decay and recovery during sample processing as well as error treatment, which relies on a range of assumptions. As a result, questions have been raised regarding the accuracy and precision of ^{210}Po and ^{210}Pb measurements in seawater (Church, *et al.*, 2012).

An initial assessment of the precision and accuracy of current procedures for ^{210}Po and ^{210}Pb measurement was conducted as part of a recent intercalibration exercise using dissolved and particulate seawater samples (Church *et al.* 2012). One of the major conclusions was that, while the results reported by laboratories agree relatively well (relative standard deviation, $\text{RSD} < 50\%$) for samples with high ^{210}Po

and ^{210}Pb activities (>0.1 dpm), this agreement became rather poor (RSD up to 200%) for lower activity samples. Although the authors were not able to precisely identify the sources of the disagreements, they suggested that one possibility includes the manner in which the ^{210}Po and ^{210}Pb ingrowth, decay and recovery calculations were conducted. Their study further revealed that there were various methodologies in how uncertainties and error propagation were considered, which resulted in a large range in the specific activity uncertainties reported. The inter-calibration effort by [Church et al. \(2012\)](#), therefore suggests that there is a need for the scientific community to concur on “best practices” for ^{210}Po and ^{210}Pb measurement as well as final data calculations.

In this context, the aims of this paper are: (1) to review the protocols used for ^{210}Po and ^{210}Pb measurements in seawater and provide recommendations for improving the method’s accuracy, (2) to detail the calculations necessary for including isotopic recoveries and decay/ingrowth corrections during sample processing, (3) to develop a protocol for error propagation and to identify the main sources of uncertainty in the final data, and (4) to recommend methods for lowering the relative uncertainty. A practical spread-sheet, which follows step wise the complex formulations reported in the paper, has been made available as an downloadable Web Appendix.

Materials and Procedures

General procedure for sample collection and processing

A typical protocol used for seawater sample processing of ^{210}Pb and ^{210}Po is presented in Figure 1 and assumes analysis of ^{210}Po and ^{210}Pb by alpha spectrometry as described by [Fleer and Bacon \(1984\)](#). The seawater sample is collected as either total (unfiltered) or dissolved (filtered) with the particulate fraction measured separately. After collection, the dissolved or total sample is acidified to pH 1-2 with HCl, spiked with a well-calibrated ^{209}Po tracer solution ($T_{1/2}=102$ y) and a well-standardized stable lead carrier added in order to monitor the losses of Po and Pb during sample processing. Some laboratories also use ^{208}Po ($T_{1/2} = 2.9$ y) in a double spike technique, the former added to monitor the initial yield and the latter to act as a second yield tracer ([Friedrich and Rutgers van der Loeff 2002](#)). In the following, we limit

our discussions to the single- ^{209}Po spike method, as tailing/peak overlap corrections for ^{208}Po (alpha energy of 5.11 MeV) and ^{210}Po (5.31 MeV) add another level of complexity not necessary for this discussion (Fleer and Bacon 1984).

For both total and dissolved samples, Po and Pb can be pre-concentrated from large volumes of seawater via co-precipitation with $\text{Fe}(\text{OH})_3$ (Thomson and Turekian 1976; Nozaki 1986), Co-APDC (Fleer and Bacon 1984) or MnO_2 (Bojanowski et al. 1983). The precipitate is then dissolved in an acid solution (generally HCl for $\text{Fe}(\text{OH})_3$ and MnO_2 , HNO_3 for Co-APDC) and, after evaporation to near-dryness, recovered in a 0.5-2M HCl solution. For particulate samples, the solid phase is completely dissolved using a mixture of strong acids (including HF) and, after evaporation to near-dryness, also recovered in 0.5-2 M HCl solution. The Po nuclides are then plated by spontaneous deposition onto a silver disc (Flynn 1968). Silver discs, typically 1-2 cm in diameter, can be obtained with greater than 99.99% purity. They are first shined with a commercial silver polish and then washed using water and ethanol. One side of the disc is covered by an inert substance, such as rubber cement, electronic spray (e.g glyptol) or plastic tape, so that Po nuclides are plated on only one side. For samples processed using $\text{Fe}(\text{OH})_3$ co-precipitation, ascorbic acid should be added to the plating solution before plating in order to avoid $\text{Fe}(\text{OH})_3$ formation on the plate. The Po activities are measured after deposition by alpha spectrometry. Any remaining ^{210}Po and ^{209}Po in solution is removed by either a second deposition onto another silver disc or scrap silver and/or using anion exchange resin such as AG-1X8 (Sarin et al. 1992) or Sr Spec resin (Vajda, et al. 1994). Note that the Po and Pb separation using Sr Spec resin can also be conducted prior to the first plating (Bojanowski et al. 1983). After separation, the final eluate containing the ^{210}Pb is re-spiked with ^{209}Po and stored for greater than 6 months to allow in-growth of ^{210}Po from ^{210}Pb . At that time, the ^{210}Pb activity of the sample is determined by replating the eluate solution on a new silver disc and measuring the in-growth of ^{210}Po (Figure 1). The determination of the initial activities of ^{210}Po and ^{210}Pb in the sample at the time of collection requires several corrections that account for decay and ingrowth between the time of collection and processing, together with corrections for Po and Pb chemical recoveries (detailed in Section 3).

Improved accuracy of the method

Use of ion exchange resin for Po and Pb separation

Complete removal of Po isotopes after the initial plating procedure is a key component for increasing the accuracy of the method. Indeed, incomplete removal of Po isotopes prior to storage will affect the final calculated ^{210}Pb activity, and thus that of ^{210}Po . There are two methods to remove the residual Po isotopes: replating the solution or separation onto ion exchange resin. Replating of samples may not be sufficient to ensure complete removal of residual Po as a fraction of the Po nuclides may remain in solution. Based on the Po recovery efficiency obtained on about 80 processed samples, we found that $17 \pm 19\%$ of the Po introduced into the plating solution can remain in solution after the first plating. Note that such results are in agreement with previous findings (Flynn 1968). Assuming the same efficiency for the cleaning plate, residual Po nuclides of $3 \pm 3\%$ will remain in solution. In contrast, ion exchange experiments with spiked solutions of known amounts of ^{209}Po and ^{210}Po showed a quantitative removal of Po ($98.9 \pm 1.4\%$, $n=6$, for AG-1X8 in HCl 9M; Rigaud unpublished results). Thus, although both methods are valid, we recommend the use of ion exchange resin in order to obtain the most accurate results.

Precise determination of ^{210}Pb recovery efficiency during sample processing

The Pb recovery is quantified by measuring stable lead concentrations in known aliquots of the plating solution. Usually only one aliquot is collected after the second plating, providing information on the total Pb loss that occurs during complete sample processing. This loss is generally assumed to occur only during sample extraction (filtered or unfiltered) or dissolution (particulate). For example experiments using the most common extraction protocols ($\text{Fe}(\text{OH})_3$ and Co-APDC methods) on about 80 dissolved seawater samples showed that the Pb extraction efficiency during initial seawater extraction were $70 \pm 10\%$ and $88 \pm 18\%$ for $\text{Fe}(\text{OH})_3$ and Co-APDC respectively. However, Pb losses have also been shown to occur during ion exchange resin procedure. For comparison, the Pb recovery during resin separation was $90 \pm 17\%$ and $96 \pm 16\%$ for the $\text{Fe}(\text{OH})_3$ and Co-APDC method respectively. Thus, although the Pb

recovery during the separation onto resin is significantly higher than during the extraction procedure, it is not always complete and can constitute a non-negligible loss of Pb during sample processing. In the case of particulate samples, for which no extraction is required (Figure 1), ion exchange separation is the main step for Pb loss during sample processing. Thus precise assessment of Pb isotope loss during both extraction and ion exchange procedure needs to be considered to accurately correct for the actual ^{210}Pb fraction that leads to ^{210}Po ingrowth between the extraction and the first plating dates as well as during the storage period. Therefore we strongly recommend collecting another aliquot of plating solution between the first plating and the resin procedure (Figure 1). Note also that the fraction of the solution removed with the aliquot, although small, must also be accounted for during the activity correction process. Indeed, the fraction of ^{210}Pb removed with the aliquot will not contribute to ^{210}Po ingrowth during the storage period, resulting in an underestimation of ^{210}Pb and an overestimation of ^{210}Po (Cf. Section 3).

Assessment

Calculations and Associated Uncertainties

In this section, calculations that correct for ^{210}Po and ^{210}Pb decay, ingrowth, and recovery are presented along with their associated assumptions. The calculations are divided into several steps that focus either on the activity of ^{210}Pb at the time of sample collection (Steps A) or ^{210}Po at the time of sample collection (Steps B). The steps are presented in Figure 2 and consider three reservoirs: (1) the sample (2) the plating solution in which Po and Pb are recovered after seawater extraction or particulate dissolution, and (3) the two silver discs (the first one for the plating of *in situ* ^{210}Po and the second one for the plating of ^{210}Po produced from the decay of ^{210}Pb during the storage period). A glossary of the terms used is presented in Table 1. We also include equations that account for the combined uncertainty calculated according to uncorrelated error propagation theory. The main sources of uncertainty we consider here are those associated with (1) the counting of ^{210}Po and ^{209}Po by alpha spectrometry, (2) the activity of the ^{209}Po spike, (3) the detector background, and (4) the Pb recovery. The uncertainties associated with the radioactive decay constants of ^{210}Po , ^{210}Pb and ^{209}Po are ignored. The uncertainties

associated with the masses of sample, the spike and carrier amounts added into the sample, the mass of the plating solution and the mass of aliquots taken for stable Pb analysis, are assumed to be of secondary importance, and thus also ignored. However, if the additions of the ^{209}Po spike and Pb carrier are made volumetrically, the volume used should be adapted to minimize uncertainties and the pipette should be repeatedly calibrated for mass using the same solution and for each analyst. An analysis of the influence of each of the uncertainties described above on the final ^{210}Po and ^{210}Pb calculated uncertainty, as well as recommendations for minimizing some of these possible sources of error, are presented in Section 4.

An Excel spread-sheet including all calculations is available as a downloadable Web Appendix. In these calculations the main assumptions are:

- (1) ^{210}Po and ^{209}Po are in chemical equilibrium at the time of co-precipitation and plating and are scavenged and plated with the same efficiency. Such isotopic equilibrium is expected to be reached after several hours of equilibration.

- (2) ^{210}Po activity on the silver discs decays only as a function of its own decay constant (i.e., ^{210}Pb is not plated onto the silver disc),

- (3) both ^{210}Po and ^{209}Po are completely removed from the plating solution after the first plating, preferably using ion exchange resin or other quantitative procedure.

- (4) ^{210}Bi is at secular equilibrium with ^{210}Pb in the sample and plating solution, and thus, the ingrowth of ^{210}Po is only function of the ^{210}Pb decay.

- (5) ^{210}Pb activity in the sample and plating solutions decrease with time as a function of its own decay constant (i.e. ^{210}Pb ingrowth from ^{226}Ra is assumed to be negligible during sample processing).

Step A: Calculation of ^{210}Pb activity and associated uncertainty in the sample

Step A-1: Calculation of ^{210}Po activity in the plating solution at the second plating date ($(A_{210\text{Po}})_{\text{sol,tplat2}}$), dpm, Eq. 1a) and its associated uncertainty ($\sigma((A_{210\text{Po}})_{\text{sol,tplat2}})$, dpm, Eq. 1b) accounting for correction of

the detector background, Po recovery and ^{210}Po decay during counting and between the dates of second plating and second counting:

$$(A_{210\text{Po}})_{\text{sol},t_{\text{plat}2}} = \left(\frac{C_{210\text{Po},2}}{T_{c2}} - (A_{210\text{Po}})_{bg,2} \right) \frac{\lambda_{210\text{Po}} T_{c2}}{1 - e^{-\lambda_{210\text{Po}} T_{c2}}} \frac{(A_{209\text{Po}})_{sp,t_{\text{cal}}} e^{-\lambda_{209\text{Po}}(t_{c2,st} - t_{sp,cal})} m_{sp2}}{\left(\frac{C_{209\text{Po},2}}{T_{c2}} - (A_{209\text{Po}})_{bg,2} \right) \frac{\lambda_{209\text{Po}} T_{c2}}{1 - e^{-\lambda_{209\text{Po}} T_{c2}}}} e^{\lambda_{210\text{Po}}(t_{c2,st} - t_{plat2})}$$

Eq. 1a

$$\sigma((A_{210\text{Po}})_{\text{sol},t_{\text{plat}2}}) =$$

$$\sqrt{\begin{aligned} & \sigma(C_{210\text{Po},2})^2 \left(\frac{\lambda_{210\text{Po}}}{1 - e^{-\lambda_{210\text{Po}} T_{c2}}} \frac{(A_{209\text{Po}})_{sp,t_{\text{cal}}} e^{-\lambda_{209\text{Po}}(t_{c2,st} - t_{sp,cal})} m_{sp2}}{\left(\frac{C_{209\text{Po},2}}{T_{c2}} - (A_{209\text{Po}})_{bg,2} \right) \frac{\lambda_{209\text{Po}} T_{c2}}{1 - e^{-\lambda_{209\text{Po}} T_{c2}}}} e^{\lambda_{210\text{Po}}(t_{c2,st} - t_{plat2})} \right)^2 \\ & + \sigma((A_{210\text{Po}})_{bg,2})^2 \left(\frac{\lambda_{210\text{Po}} T_{c2}}{1 - e^{-\lambda_{210\text{Po}} T_{c2}}} \frac{(A_{209\text{Po}})_{sp,t_{\text{cal}}} e^{-\lambda_{209\text{Po}}(t_{c2,st} - t_{sp,cal})} m_{sp2}}{\left(\frac{C_{209\text{Po},2}}{T_{c2}} - (A_{209\text{Po}})_{bg,2} \right) \frac{\lambda_{209\text{Po}} T_{c2}}{1 - e^{-\lambda_{209\text{Po}} T_{c2}}}} e^{\lambda_{210\text{Po}}(t_{c2,st} - t_{plat2})} \right)^2 \\ & + \sigma((A_{209\text{Po}})_{sp,t_{\text{cal}}})^2 \left(\left(\frac{C_{210\text{Po},2}}{T_{c2}} - (A_{210\text{Po}})_{bg,2} \right) \frac{\lambda_{210\text{Po}} T_{c2}}{1 - e^{-\lambda_{210\text{Po}} T_{c2}}} \frac{e^{-\lambda_{209\text{Po}}(t_{c2,st} - t_{sp,cal})} m_{sp2}}{\left(\frac{C_{209\text{Po},2}}{T_{c2}} - (A_{209\text{Po}})_{bg,2} \right) \frac{\lambda_{209\text{Po}} T_{c2}}{1 - e^{-\lambda_{209\text{Po}} T_{c2}}}} e^{\lambda_{210\text{Po}}(t_{c2,st} - t_{plat2})} \right)^2 \\ & + \sigma(C_{209\text{Po},2})^2 \left(\left(\frac{C_{210\text{Po},2}}{T_{c2}} - (A_{210\text{Po}})_{bg,2} \right) \frac{\lambda_{210\text{Po}} T_{c2}}{1 - e^{-\lambda_{210\text{Po}} T_{c2}}} \frac{(A_{209\text{Po}})_{sp,t_{\text{cal}}} e^{-\lambda_{209\text{Po}}(t_{c2,st} - t_{sp,cal})} m_{sp2}}{(C_{209\text{Po},2} - T_{c2}(A_{209\text{Po}})_{bg,2})^2 \frac{\lambda_{209\text{Po}}}{1 - e^{-\lambda_{209\text{Po}} T_{c2}}}} e^{\lambda_{210\text{Po}}(t_{c2,st} - t_{plat2})} \right)^2 \\ & + \sigma((A_{209\text{Po}})_{bg,2})^2 \left(\left(\frac{C_{210\text{Po},2}}{T_{c2}} - (A_{210\text{Po}})_{bg,2} \right) \frac{\lambda_{210\text{Po}} T_{c2}}{1 - e^{-\lambda_{210\text{Po}} T_{c2}}} \frac{(A_{209\text{Po}})_{sp,t_{\text{cal}}} e^{-\lambda_{209\text{Po}}(t_{c2,st} - t_{sp,cal})} m_{sp2} T_{c2}}{(C_{209\text{Po},2} - T_{c2}(A_{209\text{Po}})_{bg,2})^2 \frac{\lambda_{209\text{Po}}}{1 - e^{-\lambda_{209\text{Po}} T_{c2}}}} e^{\lambda_{210\text{Po}}(t_{c2,st} - t_{plat2})} \right)^2 \end{aligned}}$$

Eq. 1b

Note that the recovery of ^{209}Po ($f_{Po,rec2}$) during the extraction and plating steps can be used as a quality control check of sample processing. It is determined as:

$$f_{Po,rec2} = \frac{\left(\frac{C_{209\text{Po},2}}{T_{c2}} - (A_{209\text{Po}})_{bg} \right) \frac{\lambda_{209\text{Po}} T_{c2}}{1 - e^{-\lambda_{209\text{Po}} T_{c2}}}}{\varepsilon(A_{209\text{Po}})_{sp,t_{\text{cal}}} e^{-\lambda_{209\text{Po}}(t_{c2,st} - t_{sp,cal})} m_{sp2}} \quad \text{Eq. 2a}$$

Step A-2: Calculation of ^{210}Pb activity in the plating solution at the ion exchange resin separation date (($A_{210\text{Pb}})_{\text{sol},t_{\text{res}}}$, dpm, Eq. 3a) and its associated uncertainty ($\sigma((A_{210\text{Pb}})_{\text{sol},t_{\text{res}}}$, dpm, Eq. 3b) after correction for ^{210}Po in-growth and decay between the dates of resin separation and second plating:

$$(A_{210Pb})_{sol,t_{res}} = \frac{(A_{210Po})_{sol,t_{plat2}} (\lambda_{210Po} - \lambda_{210Pb})}{\lambda_{210Po} (e^{-\lambda_{210Pb}(t_{plat2}-t_{res})} - e^{-\lambda_{210Po}(t_{plat2}-t_{res})})} \quad Eq. 3a$$

$$\sigma((A_{210Pb})_{sol,t_{res}}) = \sqrt{\sigma((A_{210Po})_{sol,t_{plat2}})^2 \left(\frac{(\lambda_{210Po} - \lambda_{210Pb})}{\lambda_{210Po} (e^{-\lambda_{210Pb}(t_{plat2}-t_{res})} - e^{-\lambda_{210Po}(t_{plat2}-t_{res})})} \right)^2} \quad Eq. 3b$$

217

218 Step A-3: Calculation of ^{210}Pb activity in the sample at sampling date $((A_{210Pb})_{spl,t_{spl}}$, dpm, Eq. 4a) and its
 219 associated uncertainty $(\sigma((A_{210Pb})_{spl,t_{spl}})$, dpm, Eq. 4b) accounting for correction for ^{210}Pb decay between
 220 the dates of resin separation and sampling, Pb recoveries and blank:

$$(A_{210Pb})_{spl,t_{spl}} = \frac{(A_{210Pb})_{sol,t_{res}} e^{\lambda_{210Pb}(t_{res}-t_{spl})}}{f_{Pbrec,tot}} \left(1 + \frac{m_{al1}}{m_{sol1}} \right) - (A_{210Pb})_B \quad Eq. 4a$$

$$\sigma((A_{210Pb})_{spl,t_{spl}}) = \sqrt{\sigma((A_{210Pb})_{sol,t_{res}})^2 \left(\frac{e^{\lambda_{210Pb}(t_{res}-t_{spl})}}{f_{Pbrec,tot}} \left(1 + \frac{m_{al1}}{m_{sol1}} \right) \right)^2 + \sigma(f_{Pbrec,tot})^2 \left(\frac{(A_{210Pb})_{sol,t_{res}} e^{\lambda_{210Pb}(t_{res}-t_{spl})}}{(f_{Pbrec,tot})^2} \left(1 + \frac{m_{al1}}{m_{sol1}} \right) \right)^2 + \sigma((A_{210Pb})_B)^2} \quad Eq. 4b$$

223

224 $f_{Pbrec,tot}$ and its associated uncertainty $\sigma(f_{Pbrec,tot})$ represents the total Pb recovery efficiency during the
 225 sample processing, which includes Pb loss during the extraction from seawater samples or particulate
 226 dissolution and during the ion exchange resin separation procedure. It is obtained by :

$$f_{Pbrec,tot} = \frac{m_{sol2}[Pb]_{sol2} + m_{al1}[Pb]_{sol1}}{m_c[Pb]_c} \quad Eq. 5a$$

$$\sigma(f_{Pbrec,tot}) = \sqrt{\sigma([Pb]_{sol2})^2 \left(\frac{m_{sol2}}{m_c[Pb]_c} \right)^2 + \sigma([Pb]_{sol1})^2 \left(\frac{m_{al1}}{m_c[Pb]_c} \right)^2 + \sigma([Pb]_c)^2 \left(\frac{m_{sol2}[Pb]_{sol2} + m_{al1}[Pb]_{sol1}}{m_c[Pb]_c^2} \right)^2} \quad Eq. 5b$$

229

230 The parameters $(A_{210Pb})_B$ and $\sigma((A_{210Pb})_B)$ correspond to the activity (in dpm) and associated uncertainties,
 231 respectively, of ^{210}Pb in the blank that may be due to contamination of reagents (e.g., lead carrier). The
 232 blank is obtained by processing a volume of ultrapure water in the same manner as a sample, according to
 233 the procedure outlined in Figure 1 and calculated following steps A1 and A2, and replacing the equations
 234 of step A3 by:

$$235 \quad (A_{210Pb})_B = \frac{(A_{210Pb})_{sol,t_{res}} e^{\lambda_{210Pb}(t_{res}-t_{car})}}{f_{Pb_{rec,tot}}} \left(1 + \frac{m_{al1}}{m_{sol1}}\right) \quad Eq. 6a$$

$$236 \quad \sigma((A_{210Pb})_B) = \sqrt{\sigma((A_{210Pb})_{sol,t_{res}})^2 \left(\frac{e^{\lambda_{210Pb}(t_{res}-t_{car})}}{f_{Pb_{rec,tot}}} \left(1 + \frac{m_{al1}}{m_{sol1}}\right)\right)^2 + \sigma(f_{Pb_{rec,tot}})^2 \left(\frac{(A_{210Pb})_{sol,t_{res}} e^{\lambda_{210Pb}(t_{res}-t_{car})}}{(f_{Pb_{rec,tot}})^2} \left(1 + \frac{m_{al1}}{m_{sol1}}\right)\right)^2} \quad Eq. 6b$$

237

238 Step A-4: Final calculation of ^{210}Pb activity in the sample at the sampling date $((A_{210Pb})_{spl,t_{spl}})$ (dpm/100kg),
 239 dpm/100kg, Eq. 7a) and its associated uncertainty $(\sigma((A_{210Pb})_{spl,t_{spl}}))$ (dpm/100kg, Eq. 7b):

$$240 \quad (A_{210Pb})_{spl,t_{spl}} \left(\frac{dpm}{100kg}\right) = \frac{(A_{210Pb})_{spl,t_{spl}}}{m_{spl}} 100 \quad Eq. 7a$$

$$241 \quad \sigma\left((A_{210Pb})_{spl,t_{spl}} \left(\frac{dpm}{100kg}\right)\right) = \sqrt{\sigma\left((A_{210Pb})_{spl,t_{spl}}\right)^2 \left(\frac{100}{m_{spl}}\right)^2} \quad Eq. 7b$$

242

243 *Step B: Calculation of ^{210}Po activity and associated uncertainty in the sample*

244 Step B1: Calculation of ^{210}Po activity in the plating solution at the first plating date $((A_{210Po})_{sol,t_{plat1}})$, dpm,
 245 Eq. 8a) and its associated uncertainty $(\sigma((A_{210Po})_{sol,t_{plat1}}))$, dpm, Eq. 8b) after correction for detector
 246 background, Po recovery and ^{210}Po decay during counting and between the dates of first plating and the
 247 start of counting:

$$(A_{210Po})_{sol,t_{plat1}} = \left(\frac{C_{210Po,1}}{T_{c1}} - (A_{210Po})_{bg,1} \right) \frac{\lambda_{210Po} T_{c1}}{1 - e^{-\lambda_{210Po} T_{c1}}} \frac{(A_{209Po})_{sp,t_{cal}} e^{-\lambda_{209Po}(t_{c1,st} - t_{sp,cal})} m_{sp1}}{\left(\frac{C_{209Po,1}}{T_{c1}} - (A_{209Po})_{bg,1} \right) \frac{\lambda_{209Po} T_{c1}}{1 - e^{-\lambda_{209Po} T_{c1}}}} e^{\lambda_{210Po}(t_{c1,st} - t_{plat1})}$$

Eq. 8a

$$\sigma \left((A_{210Po})_{sol,t_{plat1}} \right) =$$

$$\sqrt{\begin{aligned} & \sigma(C_{210Po,1})^2 \left(\frac{\lambda_{210Po}}{1 - e^{-\lambda_{210Po} T_{c1}}} \frac{(A_{209Po})_{sp,t_{cal}} e^{-\lambda_{209Po}(t_{c1,st} - t_{sp,cal})} m_{sp1}}{\left(\frac{C_{209Po,1}}{T_{c1}} - (A_{209Po})_{bg,1} \right) \frac{\lambda_{209Po} T_{c1}}{1 - e^{-\lambda_{209Po} T_{c1}}}} e^{\lambda_{210Po}(t_{c1,st} - t_{plat1})} \right)^2 \\ & + \sigma((A_{210Po})_{bg,1})^2 \left(\frac{\lambda_{210Po} T_{c1}}{1 - e^{-\lambda_{210Po} T_{c1}}} \frac{(A_{209Po})_{sp,t_{cal}} e^{-\lambda_{209Po}(t_{c1,st} - t_{sp,cal})} m_{sp1}}{\left(\frac{C_{209Po,1}}{T_{c1}} - (A_{209Po})_{bg,1} \right) \frac{\lambda_{209Po} T_{c1}}{1 - e^{-\lambda_{209Po} T_{c1}}}} e^{\lambda_{210Po}(t_{c1,st} - t_{plat1})} \right)^2 \\ & + \sigma((A_{209Po})_{sp,t_{cal}})^2 \left(\left(\frac{C_{210Po,1}}{T_{c1}} - (A_{210Po})_{bg,1} \right) \frac{\lambda_{210Po} T_{c1}}{1 - e^{-\lambda_{210Po} T_{c1}}} \frac{e^{-\lambda_{209Po}(t_{c1,st} - t_{sp,cal})} m_{sp1}}{\left(\frac{C_{209Po,1}}{T_{c1}} - (A_{209Po})_{bg,1} \right) \frac{\lambda_{209Po} T_{c1}}{1 - e^{-\lambda_{209Po} T_{c1}}}} e^{\lambda_{210Po}(t_{c1,st} - t_{plat1})} \right)^2 \\ & + \sigma(C_{209Po,1})^2 \left(\left(\frac{C_{210Po,1}}{T_{c1}} - (A_{210Po})_{bg,1} \right) \frac{\lambda_{210Po} T_{c1}}{1 - e^{-\lambda_{210Po} T_{c1}}} \frac{(A_{209Po})_{sp,t_{cal}} e^{-\lambda_{209Po}(t_{c1,st} - t_{sp,cal})} m_{sp1}}{(C_{209Po,1} - T_{c1} (A_{209Po})_{bg,1})^2 \frac{\lambda_{209Po}}{1 - e^{-\lambda_{209Po} T_{c1}}}} e^{\lambda_{210Po}(t_{c1,st} - t_{plat1})} \right)^2 \\ & + \sigma((A_{209Po})_{bg,1})^2 \left(\left(\frac{C_{210Po,1}}{T_{c1}} - (A_{210Po})_{bg,1} \right) \frac{\lambda_{210Po} T_{c1}}{1 - e^{-\lambda_{210Po} T_{c1}}} \frac{(A_{209Po})_{sp,t_{cal}} e^{-\lambda_{209Po}(t_{c1,st} - t_{sp,cal})} m_{sp1} T_{c1}}{(C_{209Po,1} - T_{c1} (A_{209Po})_{bg,1})^2 \frac{\lambda_{209Po}}{1 - e^{-\lambda_{209Po} T_{c1}}}} e^{\lambda_{210Po}(t_{c1,st} - t_{plat1})} \right)^2 \end{aligned}}$$

Eq. 8b

Step B2: Calculation of ^{210}Po activity in the plating solution at the date of extraction (dissolved or total samples) or dissolution (particulate samples) $((A_{210Po})_{sol,extr}, \text{ dpm}, \text{ Eq. 9a})$ and its associated uncertainty $(\sigma((A_{210Po})_{sol,extr}), \text{ dpm}, \text{ Eq. 9b})$ after correction for ^{210}Po decay and in-growth between extraction and first plating dates:

$$\begin{aligned} & (A_{210Po})_{sol,t_{extr}} \\ & = \left((A_{210Po})_{sol,t_{plat1}} - \frac{\lambda_{210Po} \left((A_{210Pb})_{spl,t_{spl}} e^{-\lambda_{210Pb}(t_{extr} - t_{spl})} + (A_{210Pb})_B e^{-\lambda_{210Pb}(t_{extr} - t_{car})} \right) f_{Pbrec1}}{\lambda_{210Po} - \lambda_{210Pb}} \left(e^{-\lambda_{210Pb}(t_{plat1} - t_{extr})} \right. \right. \\ & \quad \left. \left. - e^{-\lambda_{210Po}(t_{plat1} - t_{extr})} \right) \right) e^{\lambda_{210Po}(t_{plat1} - t_{extr})} \end{aligned}$$

Eq. 9a

$$\begin{aligned}
& \sigma((A_{210Po})_{sol,t_{extr}}) = \\
& \sqrt{ \frac{ \sigma((A_{210Po})_{sol,t_{plat1}})^2 (e^{\lambda_{210Po}(t_{plat1}-t_{extr})})^2 }{ } } \\
& + \sigma((A_{210Pb})_{spl,t_{spl}})^2 \left(\frac{ \lambda_{210Po} e^{-\lambda_{210Pb}(t_{extr}-t_{spl})} f_{Pb_{rec1}} }{ \lambda_{210Po} - \lambda_{210Pb} } (e^{-\lambda_{210Pb}(t_{plat1}-t_{extr})} - e^{-\lambda_{210Po}(t_{plat1}-t_{extr})}) e^{\lambda_{210Po}(t_{plat1}-t_{extr})} \right)^2 \\
& + \sigma((A_{210Pb})_B)^2 \left(\frac{ \lambda_{210Po} e^{-\lambda_{210Pb}(t_{extr}-t_{car})} f_{Pb_{rec1}} }{ \lambda_{210Po} - \lambda_{210Pb} } (e^{-\lambda_{210Pb}(t_{plat1}-t_{extr})} - e^{-\lambda_{210Po}(t_{plat1}-t_{extr})}) e^{\lambda_{210Po}(t_{plat1}-t_{extr})} \right)^2 \\
& + \sigma(f_{Pb_{rec1}})^2 \left(\frac{ \lambda_{210Po} ((A_{210Pb})_{spl,t_{spl}} e^{-\lambda_{210Pb}(t_{extr}-t_{spl})} + (A_{210Pb})_B e^{-\lambda_{210Pb}(t_{extr}-t_{car})}) }{ \lambda_{210Po} - \lambda_{210Pb} } \right)^2 \\
& \left(e^{-\lambda_{210Pb}(t_{plat1}-t_{extr})} - e^{-\lambda_{210Po}(t_{plat1}-t_{extr})} \right) e^{\lambda_{210Po}(t_{plat1}-t_{extr})} \right)^2
\end{aligned}$$

Eq. 9b

$f_{Pb_{rec1}}$ and its associated uncertainty $\sigma(f_{Pb_{rec1}})$ represents the Pb recovery efficiency during sample extraction (filtered or unfiltered samples). It is obtained by :

$$f_{Pb_{rec1}} = \frac{m_{sol1}[Pb]_{sol1}}{m_c[Pb]_c} \quad Eq. 10a$$

$$\sigma(f_{Pb_{rec1}}) = \sqrt{\sigma([Pb]_{sol1})^2 \left(\frac{m_{sol1}}{m_c[Pb]_c} \right)^2 + \sigma([Pb]_c)^2 \left(\frac{m_{sol1}[Pb]_{sol1}}{m_c[Pb]_c^2} \right)^2} \quad Eq. 10b$$

Note that for particulate samples, the date of extraction (t_{extr}) in Eq. 9a and Eq. 9b should be replaced by the date of dissolution (t_{diss}), assuming that any loss of Pb that occurs during particulate sample processing is during the dissolution procedure.

Step B3: Calculation of ^{210}Po activity in the sample at sampling date ($(A_{210Po})_{sol,t_{spl}}$, dpm, Eq. 11a) and its associated uncertainty ($\sigma((A_{210Po})_{sol,t_{spl}})$, dpm, Eq. 11b) after correction for the blank and for ^{210}Po decay and in-growth between sampling date and extraction (dissolved or total) or dissolution (particulate) dates:

$$\begin{aligned}
& (A_{210Po})_{spl,t_{spl}} = (A_{210Po})_{sol,t_{extr}} e^{\lambda_{210Po}(t_{extr}-t_{spl})} \\
& - \frac{\lambda_{210Po}(A_{210Pb})_{spl,t_{spl}}}{\lambda_{210Po} - \lambda_{210Pb}} \left(e^{-\lambda_{210Pb}(t_{extr}-t_{spl})} - e^{-\lambda_{210Po}(t_{extr}-t_{spl})} \right) e^{\lambda_{210Po}(t_{extr}-t_{spl})} \\
& - \frac{\lambda_{210Po}(A_{210Pb})_B}{\lambda_{210Po} - \lambda_{210Pb}} \left(e^{-\lambda_{210Pb}(t_{extr}-t_{car})} - e^{-\lambda_{210Po}(t_{extr}-t_{car})} \right) e^{\lambda_{210Po}(t_{extr}-t_{car})} - (A_{210Po})_B
\end{aligned}$$

Eq. 11a

$$\begin{aligned}
& \sigma((A_{210Po})_{spl,t_{spl}}) \\
& = \sqrt{
\begin{aligned}
& \sigma((A_{210Po})_{sol,t_{extr}})^2 \left(e^{\lambda_{210Po}(t_{extr}-t_{spl})} \right)^2 \\
& + \sigma((A_{210Pb})_{spl,t_{spl}})^2 \left(\frac{\lambda_{210Po}}{\lambda_{210Po} - \lambda_{210Pb}} \left(e^{-\lambda_{210Pb}(t_{extr}-t_{spl})} - e^{-\lambda_{210Po}(t_{extr}-t_{spl})} \right) e^{\lambda_{210Po}(t_{extr}-t_{spl})} \right)^2 \\
& + \sigma((A_{210Pb})_B)^2 \left(\frac{\lambda_{210Po}}{\lambda_{210Po} - \lambda_{210Pb}} \left(e^{-\lambda_{210Pb}(t_{extr}-t_{car})} - e^{-\lambda_{210Po}(t_{extr}-t_{car})} \right) e^{\lambda_{210Po}(t_{extr}-t_{car})} \right)^2 \\
& + \sigma((A_{210Po})_B)^2
\end{aligned}
}
\end{aligned}$$

Eq. 11b

In the case of particulate samples, t_{extr} should be replaced by t_{diss} in Eq. 11a and Eq. 11b.

The parameters $(A_{210Po})_B$ and $\sigma((A_{210Po})_B)$ correspond to the activity and its associated uncertainty, respectively, of ^{210}Po in the blank, which should be obtained by processing a volume of ultrapure water using the same reagents as would a sample, according to the procedure outlined in Figure 1. They are calculated following step B1 and by replacing the equations of step B2 by:

$$\begin{aligned}
& (A_{210Po})_B = (A_{210Po})_{sol,t_{plat1}} e^{\lambda_{210Po}(t_{plat1}-t_{car})} \\
& - \frac{\lambda_{210Po}(A_{210Pb})_B e^{-\lambda_{210Pb}(t_{extr}-t_{car})} f_{Pbrec1}}{\lambda_{210Po} - \lambda_{210Pb}} \left(e^{-\lambda_{210Pb}(t_{plat1}-t_{extr})} \right. \\
& \left. - e^{-\lambda_{210Po}(t_{plat1}-t_{extr})} \right) e^{\lambda_{210Po}(t_{plat1}-t_{extr})} \\
& - \frac{\lambda_{210Po}(A_{210Pb})_B}{\lambda_{210Po} - \lambda_{210Pb}} \left(e^{-\lambda_{210Pb}(t_{extr}-t_{car})} - e^{-\lambda_{210Po}(t_{extr}-t_{car})} \right) e^{\lambda_{210Po}(t_{extr}-t_{car})}
\end{aligned}$$

Eq. 12a

298

$$\sigma((A_{210Po})_B) =$$

299

$$\sqrt{\begin{aligned} & \sigma((A_{210Po})_{sol,t_{plat1}})^2 (e^{\lambda_{210Po}(t_{plat1}-t_{car})})^2 \\ & + \sigma((A_{210Pb})_B)^2 \left(\frac{\lambda_{210Po} e^{-\lambda_{210Pb}(t_{extr}-t_{car})} f_{Pb_{rec1}}}{\lambda_{210Po} - \lambda_{210Pb}} (e^{-\lambda_{210Pb}(t_{plat1}-t_{extr})} - e^{-\lambda_{210Po}(t_{plat1}-t_{extr})}) e^{\lambda_{210Po}(t_{plat1}-t_{extr})} \right)^2 \\ & + \sigma((A_{210Pb})_B)^2 \left(\frac{\lambda_{210Po}}{\lambda_{210Po} - \lambda_{210Pb}} (e^{-\lambda_{210Pb}(t_{extr}-t_{car})} - e^{-\lambda_{210Po}(t_{extr}-t_{car})}) e^{\lambda_{210Po}(t_{extr}-t_{car})} \right)^2 \\ & + \sigma(f_{Pb_{rec1}})^2 \left(\frac{\lambda_{210Po}(A_{210Pb})_B e^{-\lambda_{210Pb}(t_{extr}-t_{car})}}{\lambda_{210Po} - \lambda_{210Pb}} (e^{-\lambda_{210Pb}(t_{plat1}-t_{extr})} - e^{-\lambda_{210Po}(t_{plat1}-t_{extr})}) e^{\lambda_{210Po}(t_{plat1}-t_{extr})} \right)^2 \end{aligned}}$$

300

Eq. 12b

301

302 Step B4: Final calculation of ^{210}Po activity in the sample at the sampling date $((A_{210Po})_{spl,t_{spl}} \text{ (dpm/100kg)})$,303 dpm/100kg, Eq. 13a) and its associated uncertainty $(\sigma((A_{210Po})_{spl,t_{spl}} \text{ (dpm/100kg)})$, dpm/100kg, Eq. 13b):

304

$$(A_{210Po})_{spl,t_{spl}} \left(\frac{\text{dpm}}{100\text{kg}} \right) = \frac{(A_{210Po})_{spl,t_{spl}}}{m_{spl}} 100 \quad \text{Eq. 13a}$$

305

$$\sigma((A_{210Po})_{spl,t_{spl}} \left(\frac{\text{dpm}}{100\text{kg}} \right)) = \sqrt{\sigma((A_{210Po})_{spl,t_{spl}})^2 \left(\frac{100}{m_{spl}} \right)^2} \quad \text{Eq. 13b}$$

306

307 *Step C: Calculation of the $^{210}\text{Po}/^{210}\text{Pb}$ activity ratio and associated uncertainty in the sample*308 The final $^{210}\text{Po}/^{210}\text{Pb}$ activity ratio in the sample at the sampling date $\left(\frac{(A_{210Po})_{spl,t_{spl}}}{(A_{210Pb})_{spl,t_{spl}}} \right)$ is simply obtained by309 dividing $(A_{210Po})_{spl,t_{spl}}$ (Eq. 11a) by $(A_{210Pb})_{spl,t_{spl}}$ (Eq. 4a). Its associated uncertainty $\left(\sigma \left(\frac{(A_{210Po})_{spl,t_{spl}}}{(A_{210Pb})_{spl,t_{spl}}} \right) \right)$ can be310 obtained using Eq. 14b. Note that Eq. 14b is only valid if the same ^{209}Po spike is used in steps A and B and

311 should be adapted if otherwise. Note also that for simplicity, influence of the blank in Eq. 14b was neglected.

312

313

Discussion

Influence of the relative uncertainty of individual parameters on the final ^{210}Po , ^{210}Pb and $^{210}\text{Po}/^{210}\text{Pb}$ uncertainties

The main sources of uncertainty detailed in the previous calculations are: (1) the number of counts for ^{210}Po ($C_{210\text{Po},1}$ and $C_{210\text{Po},2}$) and ^{209}Po ($C_{209\text{Po},1}$ and $C_{209\text{Po},2}$) detected by alpha spectrometry, (2) the activity of ^{209}Po in the spike ($(A_{209\text{Po}})_{sp,1cal}$), (3) the detector background for each isotope ($(A_{210\text{Po}})_{bg}$ and $(A_{209\text{Po}})_{bg}$) and (4) the estimated Pb recovery from sample processing ($f_{Pb,rec1}$ and $f_{Pb,rec,tot}$). For ^{210}Po , a fifth source of uncertainty needs to be considered that includes the error associated with ^{210}Pb , since it is used in the calculation to correct for ^{210}Po ingrowth during sample processing (i.e., Eq. 9 and Eq. 11). In this section, we report the relative influence each source of error has on the cumulative uncertainty of ^{210}Po and ^{210}Pb activities and the $^{210}\text{Po}/^{210}\text{Pb}$ activity ratio for typical experimental and environmental conditions.

The influence of a specific parameter's uncertainty on the overall uncertainty of ^{210}Po and ^{210}Pb activity, as well as the $^{210}\text{Po}/^{210}\text{Pb}$ activity ratio, is dependent on two factors: (1) the relative uncertainty of all parameters considered in the calculations, and (2) the relative weight that each parameter has in the final calculated activity. The relative uncertainty of each parameter (factor 1) is only dependent on individual experimental conditions. These include uncertainty of the spike calibration for spike activity, counting statistics for ^{209}Po and ^{210}Po in the sample and during background measurements, and on the analysis of stable Pb concentrations in the aliquots used for determining the recovery. In contrast, the relative weight of each parameter's uncertainty on the final calculated activity (factor 2) is dependent on the uncertainty calculations obtained by error propagation. These need to be precisely estimated in order to identify which parameter listed above has the most influence on the uncertainty of the final results and therefore, will provide information on areas where additional effort is needed.

We estimated the influence of the relative uncertainty of each parameter on the final calculated ^{210}Po and ^{210}Pb activities and $^{210}\text{Po}/^{210}\text{Pb}$ activity ratio based on the data obtained from ~ 200 dissolved

(<0.2 μm), particulate (>1 μm) and total (unfiltered) seawater samples collected from the North Atlantic and Pacific Oceans during GEOTRACES transects (GA-02 and GA-03) and inter-calibration cruises (Church et al. 2012). The range of values for the parameters considered within this large database (Table 2) is expected to reflect the typical range of experimental and environmental conditions that are encountered during most ^{210}Po and ^{210}Pb determinations. The influence of each parameter was tested separately (i.e.; one at a time), by using the equations presented previously and forcing the relative uncertainty of the parameter of interest to vary from 0 to 15% (range of possible values) while fixing the relative uncertainty of the other parameters at 0%. Please note that the relative uncertainty of each parameter is defined to be similar between the two steps of sample processing (Steps A: ^{210}Pb determination; Steps B: ^{210}Po determination).

Results are reported in Figure 3. Among the tested parameters, those that have the most important influence on the final uncertainty of both *in situ* ^{210}Po and ^{210}Pb activities are: (1) the calibrated ^{209}Po activity in the spike, (2) the number of counts of ^{210}Po and ^{209}Po detected by alpha spectrometry, and (3) the Pb recovery efficiency (Figure 3). The uncertainty on the number of counts of ^{210}Po and ^{209}Po and the Pb recovery efficiency has also an important influence on the final uncertainty of $^{210}\text{Po}/^{210}\text{Pb}$ activity ratio. However, it is worth noting that the uncertainty on the spike activity does not impact the final uncertainty of $^{210}\text{Po}/^{210}\text{Pb}$ activity ratio as such parameter cancel out in the $^{210}\text{Po}/^{210}\text{Pb}$ uncertainty calculation (Eq. 14b). Note that such observation is only valid if the same ^{209}Po spike is used between both steps A and B. In the case of ^{210}Po , the ^{210}Pb uncertainty also has an important influence on the final relative uncertainty (Figure 4). In contrast, the uncertainties associated with the detector backgrounds have a significantly lower influence on the final calculated ^{210}Po and ^{210}Pb activities and the $^{210}\text{Po}/^{210}\text{Pb}$ activity ratio (Figure 3). It is worth noting that, for the dataset considered, the detector backgrounds were always <5% of the ^{210}Po and ^{209}Po activities detected by individual alpha detectors.

Influence of the ^{210}Po and ^{210}Pb activities in blanks on the final ^{210}Po and ^{210}Pb activities and associated uncertainties

Reagents used during sample processing may be contaminated with ^{210}Po and ^{210}Pb and impact the final ^{210}Po and ^{210}Pb activities and $^{210}\text{Po}/^{210}\text{Pb}$ activity ratios as well as their respective uncertainties. One of the most important sources of contamination is the Pb carrier solution, which can contain significant amounts of ^{210}Po and ^{210}Pb (e.g., [Baskaran et al., 2013](#)). Based on the dataset from the typical experimental and environmental conditions stated above, we evaluate the influence of blank contamination by varying the ^{210}Po and ^{210}Pb activities in blanks between 0.00 and 0.10 dpm and assuming radioactive equilibrium between the two nuclides in blanks (Figure 5). The increase of ^{210}Po and ^{210}Pb activities in the blank results in, as expected, a decrease in the final activity on ^{210}Po and ^{210}Pb , with ^{210}Pb slightly higher than ^{210}Po . As such, it also induces a slight increase, on average, of the $^{210}\text{Po}/^{210}\text{Pb}$ activity ratio that can however induce up to 20% variation for the highest blank activity tested (Figure 5). This clearly highlights the importance of evaluating the blank contamination and to include it in the calculations.

Implications for the final uncertainty on ^{210}Po and ^{210}Pb activities and $^{210}\text{Po}/^{210}\text{Pb}$ activity ratios

In order to use ^{210}Po and ^{210}Pb as quantitative tracers for particles dynamic modeling in the ocean, the determination in seawater samples should be as precise as possible (i.e., their relative uncertainty should be as low as possible). In practice, the lowest relative uncertainties are assumed to be 3% for the ^{209}Po spike calibration, 3.5% for counting statistics and 3% for the Pb recovery and ^{210}Po and ^{210}Pb activities in the blank can be considered negligible (see next section). By applying these relative uncertainties to the typical experimental and environmental conditions stated above, the mean relative uncertainties on ^{210}Po and ^{210}Pb activities and the $^{210}\text{Po}/^{210}\text{Pb}$ activity ratio that can be obtained are $11 \pm 6\%$, $7.4 \pm 0.4\%$ and $14 \pm 7\%$, respectively. Such relative uncertainties may be considered acceptable for oceanic process modeling for ^{210}Pb . However, the higher and more variable relative uncertainties on the final calculated ^{210}Po and the $^{210}\text{Po}/^{210}\text{Pb}$ activity ratios is due to the fact that they incorporate the uncertainty of the final calculated ^{210}Pb from the ingrowth correction (cf., Eq. 9b and Eq. 11b). The extent of such a correction depends on two factors: (1) the $^{210}\text{Po}/^{210}\text{Pb}$ activity ratio in the sample (the lower the ratio, the higher the correction) and (2) the time elapsed between the sampling and the first Po plating (the

longer the time elapsed, the higher the correction). The lowest ^{210}Po relative uncertainty obtainable for the experimental conditions described is 6%, and then only obtained for those samples with a high $^{210}\text{Po}/^{210}\text{Pb}$ ratio (≥ 1) and the shortest delay between sampling and sample processing (< 80 days) (Figure 6).

Variations in sample characteristics (e.g., $^{210}\text{Po}/^{210}\text{Pb}$ activity ratio) and experimental conditions (e.g., time elapsed between sampling and first plating) can thus explain the high variability in the relative uncertainty obtained for ^{210}Po .

Comments and Recommendations

Limitation of uncertainties on in situ ^{210}Po , ^{210}Pb and $^{210}\text{Po}/^{210}\text{Pb}$ determinations

We previously identified the main sources of uncertainty in the ^{210}Po and ^{210}Pb determination. If there is no way to modify the $^{210}\text{Po}/^{210}\text{Pb}$ activity ratio in the sample, there are however several other ways to reduce the extent of the uncertainty for both ^{210}Po and ^{210}Pb and therefore $^{210}\text{Po}/^{210}\text{Pb}$ activity ratios.

Time between sampling and first plating

As the delay between the sampling and the first plating increases, the uncertainty on the ^{210}Po also increases. Therefore, it is imperative to process samples as soon as possible after collection. However, it is not always possible to practically limit this delay. This is particularly the case when considering long sampling cruises. For typical seawater samples and the experimental conditions presented previously, a delay of 3 months from time of collection at sea to first plating ashore will induce a relative uncertainty on ^{210}Po of about 7% ($^{210}\text{Po}/^{210}\text{Pb}$ activity ratio > 2), 9% ($^{210}\text{Po}/^{210}\text{Pb}$ activity ratio ~ 1) and 13% ($^{210}\text{Po}/^{210}\text{Pb}$ activity ratio ~ 0.5) (Figure 6b). In comparison, those uncertainties would be reduced to about 6% for sample processed onboard and plated within a few days after collection. Onboard processing of samples, including precipitation, filtration, dissolution/digestion and plating requires the use of specific equipment (e.g., chemical fume hoods). As research vessels continue to become more modernized, we recommend that such processing to be done onboard in order to minimize the impact of the needed corrections.

Counting statistics

One of the largest sources of uncertainty is that associated with the number of ^{210}Po and ^{209}Po counts by alpha spectrometry. The uncertainty on counting is calculated using the square root of the number of counts (e.g., [Ludwig 2003](#)), thus, the relative uncertainty on counting results decrease with an increase in the number of counts following a $y=x^{1/2}/x$ shaped-curve. Consequently, it is relatively easy to decrease this uncertainty by increasing the counting time, assuming detector backgrounds are relatively minor. For practical reasons, however, it is also necessary to balance counting periods with the number of samples that needs to be measured and counter availability. For an acceptable relative uncertainty $<3.5\%$, a minimum of ~ 820 counts is needed. For ^{210}Po , this can be obtained for a 10L dissolved seawater sample with a ^{210}Po activity of $15 \text{ dpm} \cdot 100\text{L}^{-1}$, assuming a Po recovery of 80% and a detector efficiency of 15%, in about 3 days of counting.

Spike calibration

The reported ^{209}Po activity in commercial stock solutions, from which ^{209}Po spikes are generally made, is typically certified with a relative uncertainty $< 5\%$ (e.g., a ^{209}Po solution from Eckert & Ziegler is certified at 3.1%; www.ezag.com). For the typical experimental and environmental conditions stated above, such an uncertainty can impart a 5% relative uncertainty for ^{210}Pb final activities and as much as 20% for ^{210}Po activities (Figure 3). Since the spike solution activity can vary with storage (e.g., due to evaporation) and because of the relatively high uncertainty on the ^{209}Po decay constant ($102 \pm 5\text{y}$), we recommend a regular calibration of the spike over time. Such calibrations imply the use of ^{210}Po certified standards. The use of IAEA standard RGU-1 ([IAEA 1987](#)) is recommended for such calibrations due to its low relative uncertainty on the ^{210}Po activity ($<1\%$). We also recommend the use of the same ^{209}Po spike during sample processing as it allows to significantly decrease the uncertainty on $^{210}\text{Po}/^{210}\text{Pb}$ activity ratios.

Pb recovery efficiency

The uncertainty associated with Pb recoveries is essentially dependent on that associated with the determination of stable Pb concentrations in the aliquots and carrier solution (Eq. 6b and Eq. 7b) as obtained by routine analytical techniques (e.g., atomic absorption spectrometry, [Fleer and Bacon 1984](#); [Friedrich and Rutgers van der Loeff 2002](#)). In order to reduce the uncertainty associated with this analysis, we recommend adding an amount of stable Pb to samples in sufficient quantity to ensure accurate standardization. For example, an addition of ~10 mg of Pb into the sample easily allows the Pb concentration to be determined by flame atomic absorption spectrometry (or ICPMS) with a relative uncertainty $\leq 3\%$, as this will result in Pb concentrations ranging from 5 to 15 $\mu\text{g g}^{-1}$ in a 20 times diluted 10 ml plating solution assuming a 70-95% total Pb extraction efficiency.

Blank consideration

We showed that the blank could strongly impact the ^{210}Po and ^{210}Pb activities and the $^{210}\text{Po}/^{210}\text{Pb}$ activity ratios and thus could induce an increase of their associated uncertainties. However, this essentially depends on the purity of the reagents used. One of the main sources of contamination for ^{210}Po and ^{210}Pb is the Pb carrier, which can contain significant amount of both isotopes. In order to minimize the blank, it is recommended that the carrier be made using lead obtained from ancient sources (i.e., >200y) or pure galena mineral that was shown to present the lowest ^{210}Pb activity ([Cochran et al., 1983](#)).

Summary

This paper presents methodologies for improving accuracy and precision in the determination of ^{210}Po and ^{210}Pb activities in seawater samples. This will allow one to compare data reported by different labs, and to use this isotope pair as a quantitative tracer for particle dynamics in marine systems.

First, we recommend that the accuracy of the method can be significantly improved by: (1) systematic use of ion exchange resin for Po removal after the first plating, (2) accounting for recovery of ^{210}Pb during both extraction/dissolution and ion exchange resin separation steps, (3) use of Pb yield tracer made from sufficiently old lead material (>hundred of years) or lead old mineral (e.g., galena) and (4) use

of appropriate calculations for decay/ingrowth, recovery and blank corrections, as detailed herein. We also provide as downloadable Web Appendix a spread-sheet outlining these calculations.

Second, the overall precision of the methodology is discussed by evaluating the impact of the relative uncertainty on each individual parameter included in the calculations. Parameters that have the most important influence on the final uncertainty of both *in situ* ^{210}Po and ^{210}Pb activities and thus the $^{210}\text{Po}/^{210}\text{Pb}$ activity ratio are: (1) the calibrated ^{209}Po activity in the spike, (2) the number of counts of ^{210}Po and ^{209}Po detected by alpha spectrometry, and (3) the Pb recovery efficiency. Blank contamination was also showed to increase the final relative uncertainty on ^{210}Po , ^{210}Pb and $^{210}\text{Po}/^{210}\text{Pb}$. For typical experimental and environmental conditions, such relative uncertainties are about 7% for ^{210}Pb . However, uncertainties can be considerably larger (up to 35%) for ^{210}Po , particularly for samples with low (<1) $^{210}\text{Po}/^{210}\text{Pb}$ activity ratios and when there is a long delay (>80 d) between sampling and the first Po plating. In contrast, for higher $^{210}\text{Po}/^{210}\text{Pb}$ activity ratios and shorter delays between sample collection and processing, the method described herein allows determination of the ^{210}Po activity within a 6% relative uncertainty.

491 **References**

- 492 Bacon, M. P., D. W. Spencer, and P. G. Brewer. 1976. $^{210}\text{Pb}/^{226}\text{Ra}$ and $^{210}\text{Po}/^{210}\text{Pb}$ disequilibria in
493 seawater and suspended particulate matter. *Earth Planet. Sci. Lett.* **32**: 277-296.
- 494 Baskaran, M., T. M. Church, G. Hong, A. Kumar, M. Qiang, H.-Y. Choi, S. Rigaud and K. Maiti. 2013.
495 Effects of flow rates and composition of the filter, and decay/ingrowth correction factors involved
496 with the determination of in situ particulate ^{210}Po and ^{210}Pb in seawater. *Limnol. Oceanogr. Meth.*
497 11:126-138.
- 498 Bojanowski, R., R. Fukai, S. Ballestra, and H. Asari. 1983. Determination of natural radioactive elements
499 in marine environmental materials by ion exchange and alpha spectrometry, p. 1-13. *In* I.A.E.A.
500 [ed.].
- 501 Church, T. M., S. Rigaud, M. Baskaran, A. Kumar, J. Friedrich, P. Masqué, V. Puigcorbé, G. Kim, O.
502 Radakovitch, G. Hong, H.-Y. Choi, and G. Stewart. 2012. Inter-calibration studies of ^{210}Po and
503 ^{210}Pb in dissolved and particulate sea water samples. *Limnol. Oceanogr. Meth.* **10**:776-789.
- 504 Cochran, J. K., and P. Masqué. 2003. Short-lived U/Th Series Radionuclides in the Ocean: Tracers for
505 Scavenging Rates, Export Fluxes and Particle Dynamics. *Rev. Mineral. Geochem.* **52**: 461-492.
- 506 Cochran, J. K., M. P. Bacon, S. Krishnaswami, and K. K. Turekian. 1983. ^{210}Po and ^{210}Pb distributions
507 in the central and eastern Indian Ocean. *Earth and Planetary Science Letters* **65**: 433-452.
- 508 Fleer, A. P., and M. P. Bacon. 1984. Determination of ^{210}Pb and ^{210}Po in seawater and marine
509 particulate matter. *Nucl. Instrum. Methods Phys. Res.* **223**: 243-249.
- 510 Flynn, W. W. 1968. The determination of low levels of polonium-210 in environmental materials. *Anal.*
511 *Chim. Acta* **43**: 221-227.
- 512 Friedrich, J., and M. M. Rutgers Van Der Loeff. 2002. A two-tracer (^{210}Po - ^{234}Th) approach to
513 distinguish organic carbon and biogenic silica export flux in the Antarctic Circumpolar Current.
514 *Deep-Sea Res. PT I* **49**: 101-120.
- 515 IAEA. 1987. Preparation and certification of IAEA gamma-ray spectrometry and reference materials

516 RGU-1, RGTh-1 and RGK-1, p. 48. *In* I. A. E. Agency [ed.], Technical Report IAEA/RL/148.
 517 Ludwig, K. R. 2003. Mathematical–Statistical Treatment of Data and Errors for ²³⁰Th/U Geochronology.
 518 *Rev. Mineral. Geochem.* **52**: 631-656.
 519 Masqué, P. and others 2002. Sediment accumulation rates and carbon fluxes to bottom sediments at the
 520 Western Bransfield Strait (Antarctica). *Deep Sea Research Part II: Topical Studies in*
 521 *Oceanography* **49**: 921-933.
 522 Moore, W. S., and J. Dymondt. 1988. Correlation of ²¹⁰Pb removal with organic carbon fluxes in the
 523 Pacific Ocean. *Nature* **331**: 339-341.
 524 Nozaki, Y. 1986. ²²⁶Ra-²²²Rn-²¹⁰Pb systematics in seawater near the bottom of the ocean. *Earth Planet.*
 525 *Sci. Lett.* **80**: 36-40.
 526 Nozaki, Y., J. Thomson, and K. K. Turekian. 1976. The distribution of ²¹⁰Pb and ²¹⁰Po in the surface
 527 waters of the Pacific Ocean. *Earth Planet. Sci. Lett.* **32**: 304-312.
 528 Rutgers Van Der Loeff, M. M., and W. Geibert. 2008. Chapter 7 U- and Th-Series Nuclides as Tracers of
 529 Particle Dynamics, Scavenging and Biogeochemical Cycles in the Oceans, p. 227-268. *In* S.
 530 Krishnaswami and J. K. Cochran [eds.], *Radioactivity in the Environment*. Elsevier.
 531 Rutgers van Der Loeff, M. M., and W. S. Moore. 2007. Determination of natural radioactive tracers, p.
 532 365-397. *Methods of Seawater Analysis*. Wiley-VCH Verlag GmbH.
 533 Sarin, M. M., R. Bhushan, R. Rengarajan, and D. N. Yadav. 1992. The simultaneous determination of
 534 ²³⁸U series nuclides in seawater: results from the Arabian Sea and Bay of Bengal. *Indian J. Mar.*
 535 *Sci.* **21**: 121-127.
 536 Sarin, M. M., G. Kim, and T. M. Church. 1999. ²¹⁰Po and ²¹⁰Pb in the South-equatorial Atlantic:
 537 distribution and disequilibrium in the Upper 500m. *Deep-Sea Res. PT II* **46**: 907-917.
 538 Stewart, G. M., and N. S. Fisher. 2003. Experimental studies on the accumulation of polonium-210 by
 539 marine phytoplankton. *Limnol. Oceanogr.* **48**: 9.
 540 ---. 2003. Bioaccumulation of Polonium-210 in Marine Copepods. *Limnol. Oceanogr.* **48**: 2011-2019.
 541 Stewart, G. M., S. W. Fowler, J.-L. Teyssie, O. Cotret, J. K. Cochran, and N. S. Fisher. 2005. Contrasting

542 transfer of polonium-210 and lead-210 across three trophic levels in marine plankton. *Mar. Ecol.*
543 *Prog. Ser.* **290**: 7.

544 Stewart, G. and others 2007. Comparing POC export from $^{234}\text{Th}/^{238}\text{U}$ and $^{210}\text{Po}/^{210}\text{Pb}$ disequilibria
545 with estimates from sediment traps in the northwest Mediterranean. *Deep-Sea Res. PT I* **54**:
546 1549-1570.

547 Thomson, J., and K. K. Turekian. 1976. ^{210}Po and ^{210}Pb distributions in ocean water profiles from the
548 Eastern South Pacific. *Earth Planet. Sci. Lett.* **32**: 297-303.

549 Tokieda, T., H. Narita, K. Harada, and S. Tsunogai. 1994. Sequential and rapid determination of Po-210,
550 Bi-210 and Pb-210 in natural waters. *Talanta* **41**: 2079-2085.

551 Vajda, N., J. Larosa, R. Zeisler, P. Danesi, and G. Kis-Benedek. 1997. A novel technique for the
552 simultaneous determination of ^{210}Pb and ^{210}Po using a crown ether. *J. Environ. Radioact.* **37**:
553 355-372.

554 Verdeny, E., P. Masqué, J. Garcia-Orellana, C. Hanfland, J. Kirk Cochran, and G. M. Stewart. 2009. POC
555 export from ocean surface waters by means of $^{234}\text{Th}/^{238}\text{U}$ and $^{210}\text{Po}/^{210}\text{Pb}$ disequilibria: A
556 review of the use of two radiotracer pairs. *Deep-Sea Res. PT II* **56**: 1502-1518.

557 Yang, W. F., Y. P. Huang, M. Chen, Y. S. Qiu, H. B. Li, and L. Zhang. 2011. Carbon and nitrogen
558 cycling in the Zhubi coral reef lagoon of the South China Sea as revealed by ^{210}Po and ^{210}Pb .
559 *Mar. Pollut. Bull.* **62**: 905-911.

560

Figures and Figure Legends

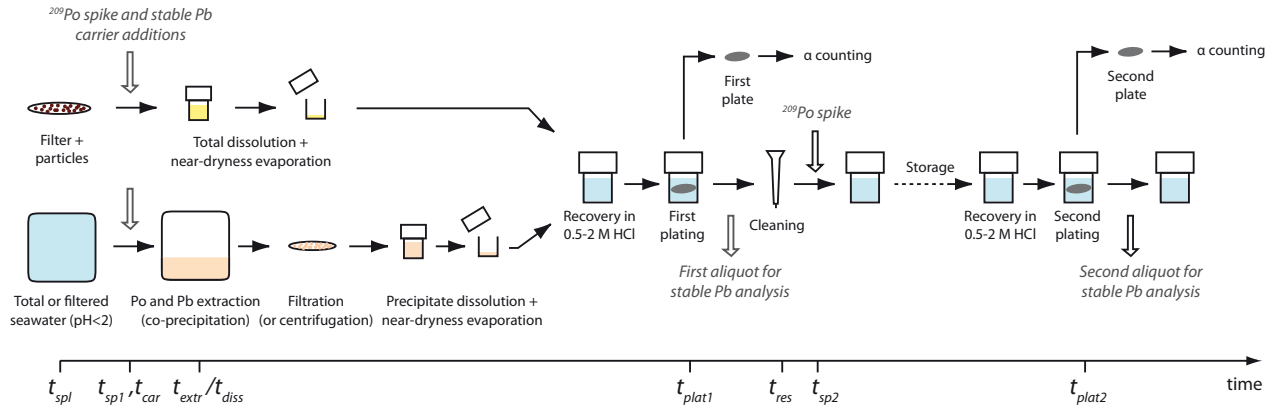


Figure 1: Sample processing scheme for the determination of total, dissolved and particulate ^{210}Po and ^{210}Pb activities. The times term (t) required for each step used in the calculation are provided.

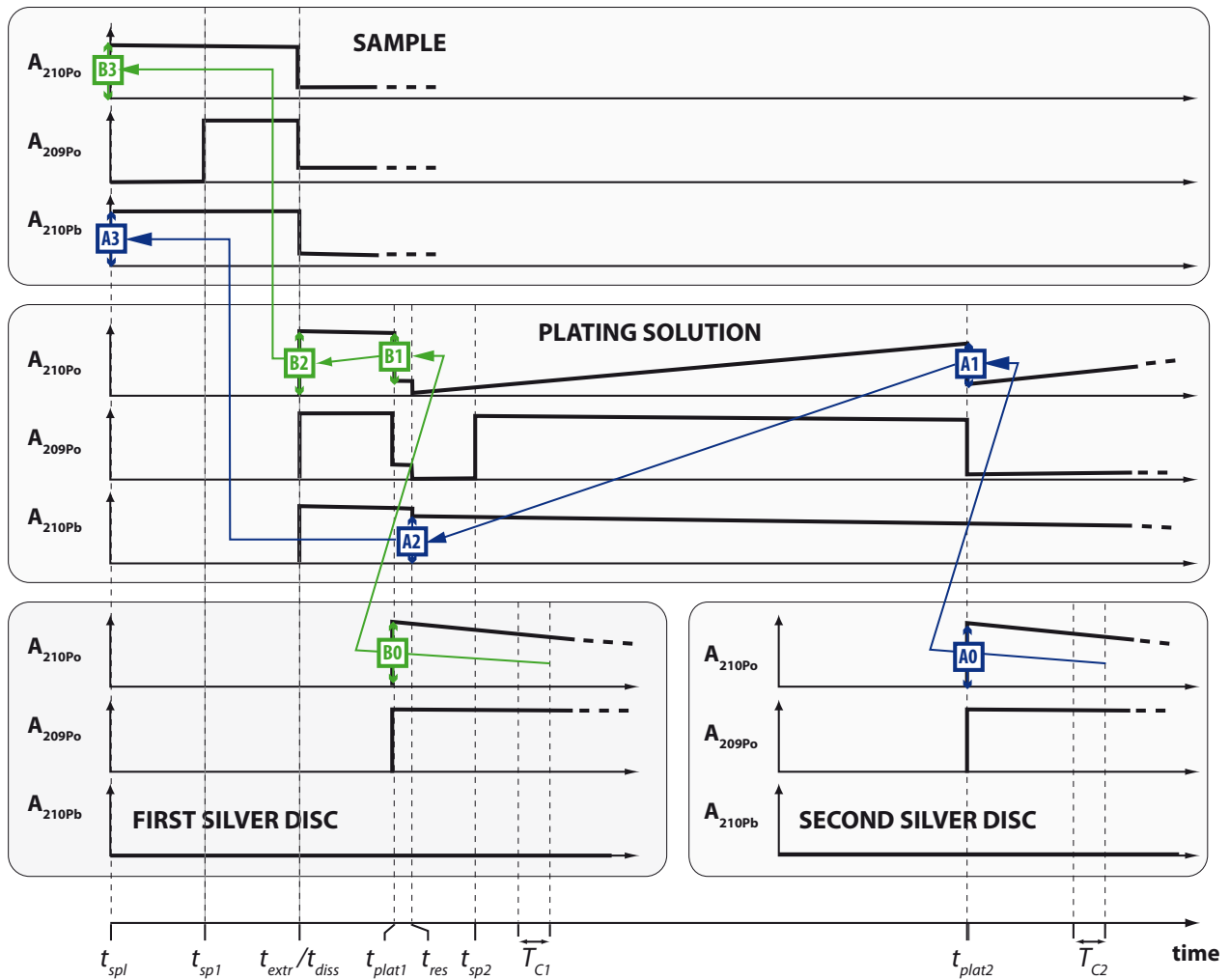


Figure 2: Schematic representation showing the temporal evolution of the activities of ^{210}Po , ^{209}Po and ^{210}Pb in the sample (total, dissolved or particulate), plating solution and silver discs during sample processing (from the left to the right). The steps followed to calculate the initial activity of ^{210}Pb (steps A) and ^{210}Po (steps B) in the sample are indicated.

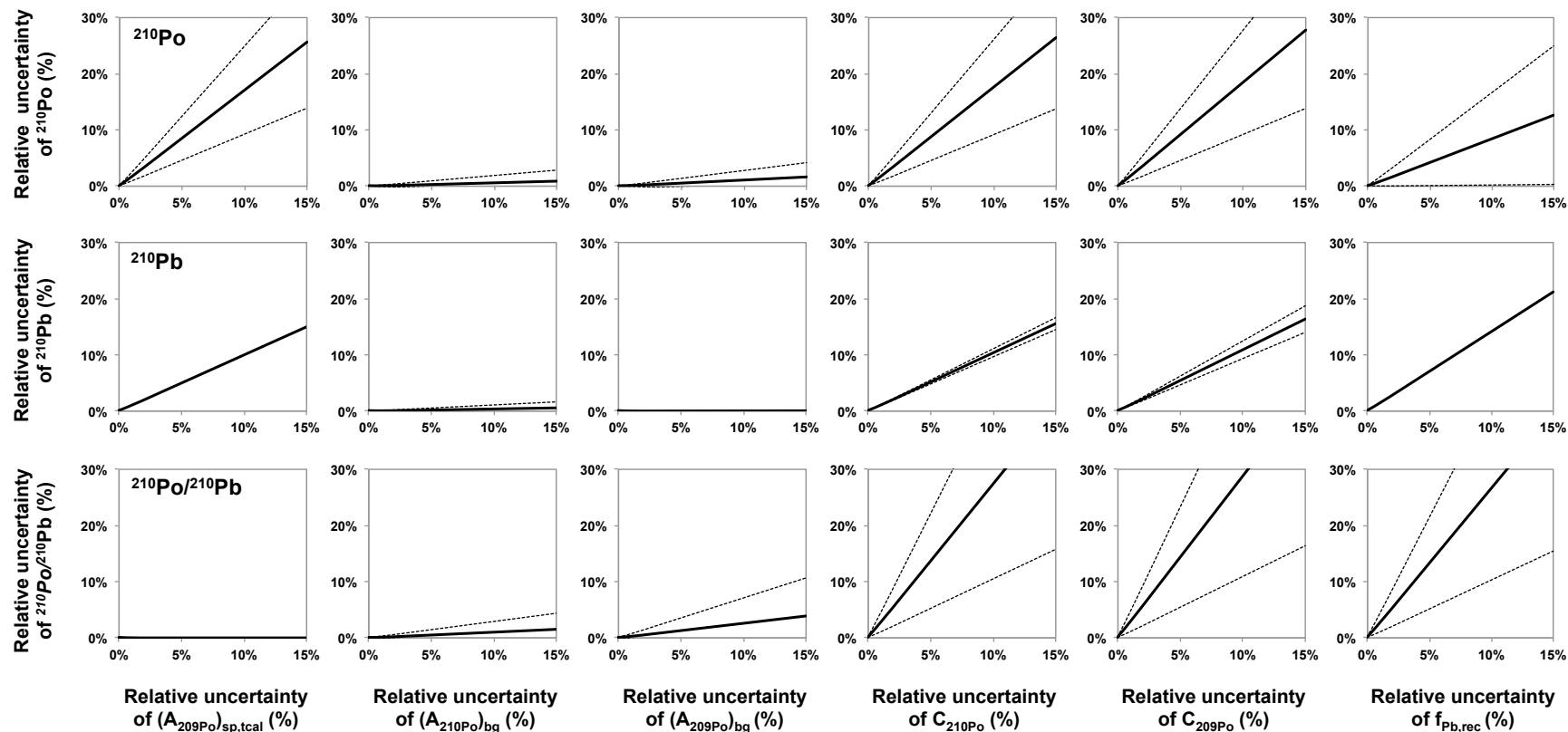


Figure 3: Evolution of the total relative uncertainty on the calculated ^{210}Po and ^{210}Pb activities and $^{210}\text{Po}/^{210}\text{Pb}$ activity ratios as a function of the relative uncertainty on parameters considered for the calculations of the activities of ^{210}Po and ^{210}Pb . The full line corresponds to the mean, and the dashed lines to the ± 1 standard deviation around the mean. They were calculated using the experimental data from the processing of 200 seawater samples by varying their individual relative uncertainty from 0 to 15%, while keeping the relative uncertainty on other parameters to 0%.

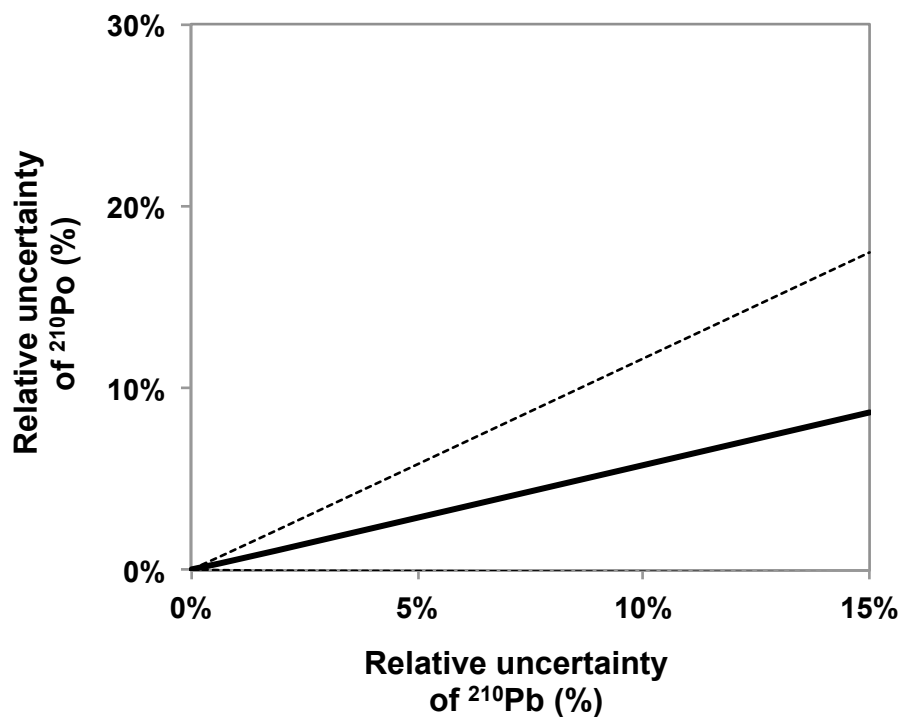


Figure 4: Evolution of the final relative uncertainty of ^{210}Po as a function of the final relative uncertainty of the ^{210}Pb activity. The full line corresponds to the mean, and the dashed lines to the ± 1 standard deviation around the mean (note that the lower dashed line can not be distinguished from the X-axis). They were calculated using the experimental data from the processing of 200 seawater samples by varying the relative uncertainty of ^{210}Pb from 0 to 15%, while keeping the relative uncertainty of all other parameters at 0%.

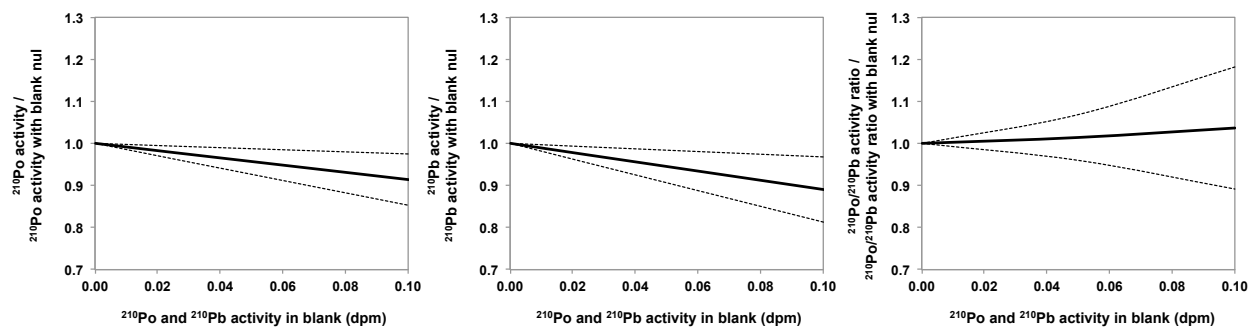


Figure 5: Influence of ^{210}Po and ^{210}Pb activities within blanks on ^{210}Po and ^{210}Pb activities and $^{210}\text{Po}/^{210}\text{Pb}$ activity ratios (expressed as the ratio between calculated values for the range of blank activity tested and the activity calculated with a null blank). The full line corresponds to the mean, and the dashed lines to the ± 1 standard deviation around the mean. They were calculated using the experimental data from the processing of 200 seawater samples.

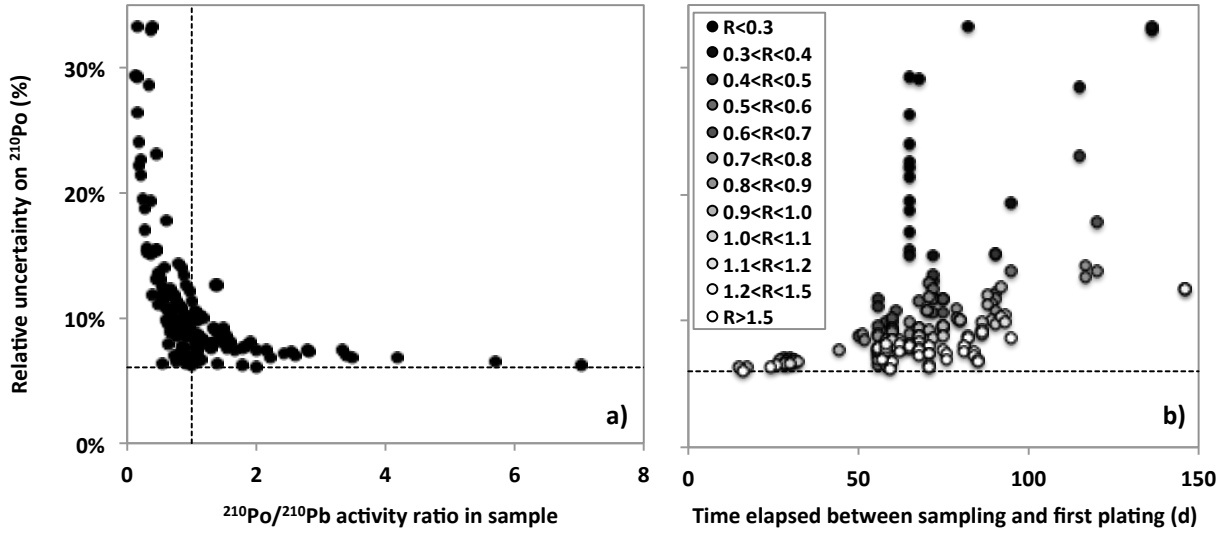


Figure 6: Relative uncertainty on the final calculated ^{210}Po activity as a function of a) $^{210}\text{Po}/^{210}\text{Pb}$ activity ratio in the sample at sampling time and b) time elapsed between sampling and first plating. These were estimated assuming relative uncertainties of 3% for the ^{209}Po spike calibration, 3.5% for the counting statistics and 3% for the Pb recovery, for the 200 samples representing typical experimental and environmental conditions presented in the text. The Y-axis is the same for both panels. The vertical dashed line represents the $^{210}\text{Po}/^{210}\text{Pb}$ activity ratio of 1. The horizontal dashed line represents the lowest ^{210}Po relative uncertainty obtained under these conditions, 6%. R corresponds to the $^{210}\text{Po}/^{210}\text{Pb}$ activity ratio. In b), the data with high (>13%) relative uncertainty on ^{210}Po and plated 65-70 days after collection, correspond to samples with quite low $^{210}\text{Po}/^{210}\text{Pb}$ activity ratios (<0.3) and were mostly dissolved surface samples from different stations, that were by chance processed with similar time delays.

Tables

Table 1: List of parameters used in the calculations with their dimension and definition

Parameter	Dimension	Definition
CONSTANTS		
λ_{210Pb}	min^{-1}	^{210}Pb decay constant
λ_{209Po}	min^{-1}	^{209}Po decay constant
λ_{210Po}	min^{-1}	^{210}Po decay constant
SAMPLE INFORMATION		
t_{spl}		Sampling date
m_{spl}	kg	Mass of the sample.
DETECTOR INFORMATION		
ε		Detector efficiency
$(A_{210Po})_{bg,1}$ and $(A_{210Po})_{bg,2}$	cpm	First and second detector background for ^{210}Po
$(A_{209Po})_{bg,1}$ and $(A_{209Po})_{bg,2}$	cpm	First and second detector background for ^{209}Po
PROCESSING & ANALYSIS INFORMATION		
t_{spl} and t_{sp2}		First and second spike addition dates
t_{extr} and t_{diss}		Extraction (filtered or unfiltered samples) or dissolution (particulate samples) dates
t_{plat1} and t_{plat2}		First and second plating dates
$t_{c1,st}$ and $t_{c2,st}$		Starting dates of the first and second counting
T_{C1} or T_{C2}	min	First and second counting times
t_{res}		Resin separation date
t_{car}		Carrier addition date
$t_{sp,cal}$		^{209}Po spike calibration date
m_{sp1} and m_{sp2}	g	First and second masses of the ^{209}Po spikes added
$C_{210Po,1}$ and $C_{210Po,2}$	cp	Total counts of ^{210}Po during the first and second counting
$C_{209Po,1}$ and $C_{209Po,2}$	cp	Total counts of ^{209}Po during the first and second counting
$(A_{209Po})_{sp,t_{cal}}$	$\text{dpm}\cdot\text{g}^{-1}$	^{209}Po activity in the spike at the date of calibration
m_{a11}	g	Mass of the first aliquot of the plating solution collected after the first plating for stable Pb analysis.
m_c	g	Mass of Pb carrier solution added in the sample.
m_{sol1} and m_{sol2}	g	Mass of the plating solution when the first and second aliquots for stable Pb analysis were collected
$[Pb]_c$, $[Pb]_{sol1}$ and $[Pb]_{sol2}$	$\mu\text{g}\cdot\text{g}^{-1}$	Pb concentration in the carrier solution and in the plating solution when the first and second aliquots for stable Pb analysis were collected
CALCULATED PARAMETERS		
$f_{Po,rec1}$ and $f_{Po,rec2}$		First and second Po recovery efficiencies
$f_{Pb,rec1}$ and $f_{Pb,rec_{tot}}$		Pb recovery efficiencies during extraction/dissolution only and during total sample processing (including also resin separation step) respectively
$(A_{210Po})_B$ and $(A_{210Pb})_B$	dpm	^{210}Po and ^{210}Pb activity in the blank, corresponding to their respective activity brought with carrier addition
$(A_{210Po})_{sol,t_{plat1}}$ and $(A_{210Po})_{sol,t_{plat2}}$	dpm	^{210}Po activity in the plating solution at the first and second plating dates respectively
$(A_{210Pb})_{sol,t_{res}}$	dpm	^{210}Pb activity in the plating solution at the resin separation date
$(A_{210Po})_{sol,t_{extr}}$ and $(A_{210Po})_{sol,t_{diss}}$	dpm	^{210}Po activity in the plating solution at the extraction (filtered or unfiltered samples) or dissolution (particulate samples) dates
$(A_{210Pb})_{spl,t_{spl}}$ and $(A_{210Po})_{spl,t_{spl}}$	dpm	^{210}Pb and ^{210}Po activity in the sample at the sampling date
$(A_{210Pb})_{spl,t_{spl}} \left(\frac{\text{dpm}}{100\text{kg}}\right)$ and $(A_{210Po})_{spl,t_{spl}} \left(\frac{\text{dpm}}{100\text{kg}}\right)$	$\text{dpm}\cdot 100\text{kg}^{-1}$	^{210}Pb and ^{210}Po activity in the sample at the sampling date

Table 2: Range of values for the parameters considered for typical experimental and environmental conditions. These originate from about 200 data representing dissolved, particulate or total seawater samples processed for ^{210}Po and ^{210}Pb determination.

Considered parameters in the uncertainty calculation*	Range of reported values (n=189)
$(A_{209\text{Po}})_{\text{sp,cal}}$ (dpm/g)	1.3-53.4
$(A_{210\text{Po}})_{\text{bg}}$ (dpm)	<0.001-0.014
$(A_{209\text{Po}})_{\text{bg}}$ (dpm)	<0.001-0.047
$C_{210\text{Po}}$ (counts)	100-2700
$C_{209\text{Po}}$ (counts)	130-6700
$f_{\text{Pb,rec}}$ (%)	15-112

*parameters from the steps A and B of samples processing are here combined

A methods assessment and recommendations for improving calculations and reducing uncertainties in the determination of ^{210}Po and ^{210}Pb activities in seawater

S. Rigaud¹, V. Puigcorbé^{2,3}, P. Cámara-Mor^{2,3}, N. Casacuberta^{2,3}, M. Roca-Martí^{2,3}, J. Garcia-Orellana^{2,3}, C. R. Benitez-Nelson⁴, P. Masqué^{2,3}, and T. Church¹

¹School of Marine Science and Policy, University of Delaware, Newark, Delaware 19716 USA.

²Departament de Física, Universitat Autònoma de Barcelona, Barcelona 08193 Spain.

³Institut de Ciència i Tecnologia Ambientals, Universitat Autònoma de Barcelona, Barcelona 08193 Spain.

⁴Marine Science Program and Department of Earth and Ocean Sciences, University of South Carolina, South Carolina 29208 USA.

Equations Appendix A

Eq. 1a

$$(A_{210\text{Po}})_{\text{sol},t_{\text{plat}2}} = \left(\frac{C_{210\text{Po},2}}{T_{c2}} - (A_{210\text{Po}})_{\text{bg},2} \right) \frac{\lambda_{210\text{Po}} T_{c2}}{1 - e^{-\lambda_{210\text{Po}} T_{c2}}} \frac{(A_{209\text{Po}})_{\text{sp},t_{\text{cal}}} e^{-\lambda_{209\text{Po}}(t_{c2,\text{st}} - t_{\text{sp},\text{cal}})} m_{\text{sp}2}}{\left(\frac{C_{209\text{Po},2}}{T_{c2}} - (A_{209\text{Po}})_{\text{bg},2} \right) \frac{\lambda_{209\text{Po}} T_{c2}}{1 - e^{-\lambda_{209\text{Po}} T_{c2}}}} e^{\lambda_{210\text{Po}}(t_{c2,\text{st}} - t_{\text{plat}2})}$$

Eq. 1b

$$\begin{aligned}
\sigma((A_{210Po})_{sol,t_{plat2}}) = & \sqrt{ \left(\sigma(C_{210Po,2})^2 \left(\frac{\lambda_{210Po}}{1 - e^{-\lambda_{210Po}T_{c2}}} \frac{(A_{209Po})_{sp,t_{cal}} e^{-\lambda_{209Po}(t_{c2,st}-t_{sp,cal})} m_{sp2}}{\left(\frac{C_{209Po,2}}{T_{c2}} - (A_{209Po})_{bg,2} \right) \frac{\lambda_{209Po}T_{c2}}{1 - e^{-\lambda_{209Po}T_{c2}}}} e^{\lambda_{210Po}(t_{c2,st}-t_{plat2})} \right)^2 \right. \\
& + \sigma((A_{210Po})_{bg,2})^2 \left(\frac{\lambda_{210Po}T_{c2}}{1 - e^{-\lambda_{210Po}T_{c2}}} \frac{(A_{209Po})_{sp,t_{cal}} e^{-\lambda_{209Po}(t_{c2,st}-t_{sp,cal})} m_{sp2}}{\left(\frac{C_{209Po,2}}{T_{c2}} - (A_{209Po})_{bg,2} \right) \frac{\lambda_{209Po}T_{c2}}{1 - e^{-\lambda_{209Po}T_{c2}}}} e^{\lambda_{210Po}(t_{c2,st}-t_{plat2})} \right)^2 \\
& + \sigma((A_{209Po})_{sp,t_{cal}})^2 \left(\left(\frac{C_{210Po,2}}{T_{c2}} - (A_{210Po})_{bg,2} \right) \frac{\lambda_{210Po}T_{c2}}{1 - e^{-\lambda_{210Po}T_{c2}}} \frac{e^{-\lambda_{209Po}(t_{c2,st}-t_{sp,cal})} m_{sp2}}{\left(\frac{C_{209Po,2}}{T_{c2}} - (A_{209Po})_{bg,2} \right) \frac{\lambda_{209Po}T_{c2}}{1 - e^{-\lambda_{209Po}T_{c2}}}} e^{\lambda_{210Po}(t_{c2,st}-t_{plat2})} \right)^2 \\
& + \sigma(C_{209Po,2})^2 \left(\left(\frac{C_{210Po,2}}{T_{c2}} - (A_{210Po})_{bg,2} \right) \frac{\lambda_{210Po}T_{c2}}{1 - e^{-\lambda_{210Po}T_{c2}}} \frac{(A_{209Po})_{sp,t_{cal}} e^{-\lambda_{209Po}(t_{c2,st}-t_{sp,cal})} m_{sp2}}{\left(C_{209Po,2} - T_{c2}(A_{209Po})_{bg,2} \right)^2 \frac{\lambda_{209Po}}{1 - e^{-\lambda_{209Po}T_{c2}}}} e^{\lambda_{210Po}(t_{c2,st}-t_{plat2})} \right)^2 \\
& \left. + \sigma((A_{209Po})_{bg,2})^2 \left(\left(\frac{C_{210Po,2}}{T_{c2}} - (A_{210Po})_{bg,2} \right) \frac{\lambda_{210Po}T_{c2}}{1 - e^{-\lambda_{210Po}T_{c2}}} \frac{(A_{209Po})_{sp,t_{cal}} e^{-\lambda_{209Po}(t_{c2,st}-t_{sp,cal})} m_{sp2}T_{c2}}{\left(C_{209Po,2} - T_{c2}(A_{209Po})_{bg,2} \right)^2 \frac{\lambda_{209Po}}{1 - e^{-\lambda_{209Po}T_{c2}}}} e^{\lambda_{210Po}(t_{c2,st}-t_{plat2})} \right)^2 \right)
\end{aligned}$$

Eq. 2a

$$f_{Po_{rec2}} = \frac{\left(\frac{C_{209Po,2}}{T_{c2}} - (A_{209Po})_{bg} \right) \frac{\lambda_{209Po}T_{c2}}{1 - e^{-\lambda_{209Po}T_{c2}}}}{\varepsilon(A_{209Po})_{sp,t_{cal}} e^{-\lambda_{209Po}(t_{c2,st}-t_{sp,cal})} m_{sp2}}$$

Eq. 3a

$$(A_{210Pb})_{sol,t_{res}} = \frac{(A_{210Po})_{sol,t_{plat2}}(\lambda_{210Po} - \lambda_{210Pb})}{\lambda_{210Po}(e^{-\lambda_{210Pb}(t_{plat2}-t_{res})} - e^{-\lambda_{210Po}(t_{plat2}-t_{res})})}$$

Eq. 3b

$$\sigma((A_{210Pb})_{sol,t_{res}}) = \sqrt{\sigma((A_{210Po})_{sol,t_{plat2}})^2 \left(\frac{(\lambda_{210Po} - \lambda_{210Pb})}{\lambda_{210Po}(e^{-\lambda_{210Pb}(t_{plat2}-t_{res})} - e^{-\lambda_{210Po}(t_{plat2}-t_{res})})} \right)^2}$$

Eq. 4a

$$(A_{210Pb})_{spl,t_{spl}} = \frac{(A_{210Pb})_{sol,t_{res}} e^{\lambda_{210Pb}(t_{res}-t_{spl})}}{f_{Pb_{rec,tot}}} \left(1 + \frac{m_{al1}}{m_{sol1}} \right) - (A_{210Pb})_B$$

Eq. 4b

$$\sigma((A_{210Pb})_{spl,t_{spl}}) = \sqrt{\sigma((A_{210Pb})_{sol,t_{res}})^2 \left(\frac{e^{\lambda_{210Pb}(t_{res}-t_{spl})}}{f_{Pb_{rec,tot}}} \left(1 + \frac{m_{al1}}{m_{sol1}} \right) \right)^2 + \sigma(f_{Pb_{rec,tot}})^2 \left(\frac{(A_{210Pb})_{sol,t_{res}} e^{\lambda_{210Pb}(t_{res}-t_{spl})}}{(f_{Pb_{rec,tot}})^2} \left(1 + \frac{m_{al1}}{m_{sol1}} \right) \right)^2 + \sigma((A_{210Pb})_B)^2}$$

Eq. 5a

$$f_{Pb_{rec,tot}} = \frac{m_{sol2}[Pb]_{sol2} + m_{al1}[Pb]_{sol1}}{m_c[Pb]_c}$$

Eq. 5b

$$\sigma(f_{Pb_{rec,tot}}) = \sqrt{\begin{aligned} &\sigma([Pb]_{sol2})^2 \left(\frac{m_{sol2}}{m_c[Pb]_c}\right)^2 \\ &+ \sigma([Pb]_{sol1})^2 \left(\frac{m_{al1}}{m_c[Pb]_c}\right)^2 \\ &+ \sigma([Pb]_c)^2 \left(\frac{m_{sol2}[Pb]_{sol2} + m_{al1}[Pb]_{sol1}}{m_c[Pb]_c^2}\right)^2 \end{aligned}}$$

Eq. 6a

$$(A_{210Pb})_B = \frac{(A_{210Pb})_{sol,t_{res}} e^{\lambda_{210Pb}(t_{res}-t_{car})}}{f_{Pb_{rec,tot}}} \left(1 + \frac{m_{al1}}{m_{sol1}}\right)$$

Eq. 6b

$$\sigma((A_{210Pb})_B) = \sqrt{\begin{aligned} &\sigma((A_{210Pb})_{sol,t_{res}})^2 \left(\frac{e^{\lambda_{210Pb}(t_{res}-t_{car})}}{f_{Pb_{rec,tot}}} \left(1 + \frac{m_{al1}}{m_{sol1}}\right)\right)^2 \\ &+ \sigma(f_{Pb_{rec,tot}})^2 \left(\frac{(A_{210Pb})_{sol,t_{res}} e^{\lambda_{210Pb}(t_{res}-t_{car})}}{(f_{Pb_{rec,tot}})^2} \left(1 + \frac{m_{al1}}{m_{sol1}}\right)\right)^2 \end{aligned}}$$

Eq. 7a

$$(A_{210Pb})_{spl,t_{spl}} \left(\frac{dpm}{100kg} \right) = \frac{(A_{210Pb})_{spl,t_{spl}}}{m_{spl}} 100$$

Eq. 7b

$$\sigma \left((A_{210Pb})_{spl,t_{spl}} \left(\frac{dpm}{100kg} \right) \right) = \sqrt{\sigma \left((A_{210Pb})_{spl,t_{spl}} \right)^2 \left(\frac{100}{m_{spl}} \right)^2}$$

Eq. 8a

$$(A_{210Po})_{sol,t_{plat1}} = \left(\frac{C_{210Po,1}}{T_{c1}} - (A_{210Po})_{bg,1} \right) \frac{\lambda_{210Po} T_{c1}}{1 - e^{-\lambda_{210Po} T_{c1}}} \frac{(A_{209Po})_{sp,t_{cal}} e^{-\lambda_{209Po}(t_{c1,st} - t_{sp,cal})} m_{sp1}}{\left(\frac{C_{209Po,1}}{T_{c1}} - (A_{209Po})_{bg,1} \right) \frac{\lambda_{209Po} T_{c1}}{1 - e^{-\lambda_{209Po} T_{c1}}}} e^{\lambda_{210Po}(t_{c1,st} - t_{plat1})}$$

Eq. 8b

$$\sigma((A_{210Po})_{sol,t_{plat1}}) = \sqrt{\begin{aligned} & \sigma(C_{210Po,1})^2 \left(\frac{\lambda_{210Po}}{1 - e^{-\lambda_{210Po}T_{c1}}} \frac{(A_{209Po})_{sp,t_{cal}} e^{-\lambda_{209Po}(t_{c1,st}-t_{sp,cal})} m_{sp1}}{\left(\frac{C_{209Po,1}}{T_{c1}} - (A_{209Po})_{bg,1}\right) \frac{\lambda_{209Po}T_{c1}}{1 - e^{-\lambda_{209Po}T_{c1}}}} e^{\lambda_{210Po}(t_{c1,st}-t_{plat1})} \right)^2 \\ & + \sigma((A_{210Po})_{bg,1})^2 \left(\frac{\lambda_{210Po}T_{c1}}{1 - e^{-\lambda_{210Po}T_{c1}}} \frac{(A_{209Po})_{sp,t_{cal}} e^{-\lambda_{209Po}(t_{c1,st}-t_{sp,cal})} m_{sp1}}{\left(\frac{C_{209Po,1}}{T_{c1}} - (A_{209Po})_{bg,1}\right) \frac{\lambda_{209Po}T_{c1}}{1 - e^{-\lambda_{209Po}T_{c1}}}} e^{\lambda_{210Po}(t_{c1,st}-t_{plat1})} \right)^2 \\ & + \sigma((A_{209Po})_{sp,t_{cal}})^2 \left(\left(\frac{C_{210Po,1}}{T_{c1}} - (A_{210Po})_{bg,1}\right) \frac{\lambda_{210Po}T_{c1}}{1 - e^{-\lambda_{210Po}T_{c1}}} \frac{e^{-\lambda_{209Po}(t_{c1,st}-t_{sp,cal})} m_{sp1}}{\left(\frac{C_{209Po,1}}{T_{c1}} - (A_{209Po})_{bg,1}\right) \frac{\lambda_{209Po}T_{c1}}{1 - e^{-\lambda_{209Po}T_{c1}}}} e^{\lambda_{210Po}(t_{c1,st}-t_{plat1})} \right)^2 \\ & + \sigma(C_{209Po,1})^2 \left(\left(\frac{C_{210Po,1}}{T_{c1}} - (A_{210Po})_{bg,1}\right) \frac{\lambda_{210Po}T_{c1}}{1 - e^{-\lambda_{210Po}T_{c1}}} \frac{(A_{209Po})_{sp,t_{cal}} e^{-\lambda_{209Po}(t_{c1,st}-t_{sp,cal})} m_{sp1}}{(C_{209Po,1} - T_{c1}(A_{209Po})_{bg,1})^2 \frac{\lambda_{209Po}}{1 - e^{-\lambda_{209Po}T_{c1}}}} e^{\lambda_{210Po}(t_{c1,st}-t_{plat1})} \right)^2 \\ & + \sigma((A_{209Po})_{bg,1})^2 \left(\left(\frac{C_{210Po,1}}{T_{c1}} - (A_{210Po})_{bg,1}\right) \frac{\lambda_{210Po}T_{c1}}{1 - e^{-\lambda_{210Po}T_{c1}}} \frac{(A_{209Po})_{sp,t_{cal}} e^{-\lambda_{209Po}(t_{c1,st}-t_{sp,cal})} m_{sp1}T_{c1}}{(C_{209Po,1} - T_{c1}(A_{209Po})_{bg,1})^2 \frac{\lambda_{209Po}}{1 - e^{-\lambda_{209Po}T_{c1}}}} e^{\lambda_{210Po}(t_{c1,st}-t_{plat1})} \right)^2 \end{aligned}}$$

Eq. 9a

$$\begin{aligned} (A_{210Po})_{sol,t_{extr}} = & \left((A_{210Po})_{sol,t_{plat1}} - \frac{\lambda_{210Po} \left((A_{210Pb})_{spl,t_{spl}} e^{-\lambda_{210Pb}(t_{extr}-t_{spl})} + (A_{210Pb})_B e^{-\lambda_{210Pb}(t_{extr}-t_{car})} \right) f_{Pb_{rec1}}}{\lambda_{210Po} - \lambda_{210Pb}} \left(e^{-\lambda_{210Pb}(t_{plat1}-t_{extr})} \right. \right. \\ & \left. \left. - e^{-\lambda_{210Po}(t_{plat1}-t_{extr})} \right) \right) e^{\lambda_{210Po}(t_{plat1}-t_{extr})} \end{aligned}$$

Eq. 9b

$$\sigma((A_{210Po})_{sol,t_{extr}}) = \sqrt{\begin{aligned} & \sigma((A_{210Po})_{sol,t_{plat1}})^2 (e^{\lambda_{210Po}(t_{plat1}-t_{extr})})^2 \\ & + \sigma((A_{210Pb})_{spl,t_{spl}})^2 \left(\frac{\lambda_{210Po} e^{-\lambda_{210Pb}(t_{extr}-t_{spl})} f_{Pb_{rec1}}}{\lambda_{210Po} - \lambda_{210Pb}} (e^{-\lambda_{210Pb}(t_{plat1}-t_{extr})} - e^{-\lambda_{210Po}(t_{plat1}-t_{extr})}) e^{\lambda_{210Po}(t_{plat1}-t_{extr})} \right)^2 \\ & + \sigma((A_{210Pb})_B)^2 \left(\frac{\lambda_{210Po} e^{-\lambda_{210Pb}(t_{extr}-t_{car})} f_{Pb_{rec1}}}{\lambda_{210Po} - \lambda_{210Pb}} (e^{-\lambda_{210Pb}(t_{plat1}-t_{extr})} - e^{-\lambda_{210Po}(t_{plat1}-t_{extr})}) e^{\lambda_{210Po}(t_{plat1}-t_{extr})} \right)^2 \\ & + \sigma(f_{Pb_{rec1}})^2 \left(\frac{\lambda_{210Po} ((A_{210Pb})_{spl,t_{spl}} e^{-\lambda_{210Pb}(t_{extr}-t_{spl})} + (A_{210Pb})_B e^{-\lambda_{210Pb}(t_{extr}-t_{car})})}{(\lambda_{210Po} - \lambda_{210Pb}) (e^{-\lambda_{210Pb}(t_{plat1}-t_{extr})} - e^{-\lambda_{210Po}(t_{plat1}-t_{extr})}) e^{\lambda_{210Po}(t_{plat1}-t_{extr})}} \right)^2 \end{aligned}}$$

Eq. 10a

$$f_{Pb_{rec1}} = \frac{m_{sol1}[Pb]_{sol1}}{m_c[Pb]_c}$$

Eq. 10b

$$\sigma(f_{Pb_{rec1}}) = \sqrt{\sigma([Pb]_{sol1})^2 \left(\frac{m_{sol1}}{m_c[Pb]_c} \right)^2 + \sigma([Pb]_c)^2 \left(\frac{m_{sol1}[Pb]_{sol1}}{m_c[Pb]_c^2} \right)^2}$$

Eq. 11a

$$(A_{210Po})_{spl,t_{spl}} = (A_{210Po})_{sol,t_{extr}} e^{\lambda_{210Po}(t_{extr}-t_{spl})} - \frac{\lambda_{210Po}(A_{210Pb})_{spl,t_{spl}}}{\lambda_{210Po} - \lambda_{210Pb}} \left(e^{-\lambda_{210Pb}(t_{extr}-t_{spl})} - e^{-\lambda_{210Po}(t_{extr}-t_{spl})} \right) e^{\lambda_{210Po}(t_{extr}-t_{spl})}$$

$$- \frac{\lambda_{210Po}(A_{210Pb})_B}{\lambda_{210Po} - \lambda_{210Pb}} \left(e^{-\lambda_{210Pb}(t_{extr}-t_{car})} - e^{-\lambda_{210Po}(t_{extr}-t_{car})} \right) e^{\lambda_{210Po}(t_{extr}-t_{car})} - (A_{210Po})_B$$

Eq. 11b

$$\sigma \left((A_{210Po})_{spl,t_{spl}} \right) = \sqrt{\begin{aligned} & \sigma \left((A_{210Po})_{sol,t_{extr}} \right)^2 \left(e^{\lambda_{210Po}(t_{extr}-t_{spl})} \right)^2 \\ & + \sigma \left((A_{210Pb})_{spl,t_{spl}} \right)^2 \left(\frac{\lambda_{210Po}}{\lambda_{210Po} - \lambda_{210Pb}} \left(e^{-\lambda_{210Pb}(t_{extr}-t_{spl})} - e^{-\lambda_{210Po}(t_{extr}-t_{spl})} \right) e^{\lambda_{210Po}(t_{extr}-t_{spl})} \right)^2 \\ & + \sigma \left((A_{210Pb})_B \right)^2 \left(\frac{\lambda_{210Po}}{\lambda_{210Po} - \lambda_{210Pb}} \left(e^{-\lambda_{210Pb}(t_{extr}-t_{car})} - e^{-\lambda_{210Po}(t_{extr}-t_{car})} \right) e^{\lambda_{210Po}(t_{extr}-t_{car})} \right)^2 \\ & + \sigma \left((A_{210Po})_B \right)^2 \end{aligned}}$$

Eq. 12a

$$(A_{210Po})_B = (A_{210Po})_{sol,t_{plat1}} e^{\lambda_{210Po}(t_{plat1}-t_{car})} - \frac{\lambda_{210Po}(A_{210Pb})_B e^{-\lambda_{210Pb}(t_{extr}-t_{car})} f_{Pb_{rec1}}}{\lambda_{210Po} - \lambda_{210Pb}} \left(e^{-\lambda_{210Pb}(t_{plat1}-t_{extr})} - e^{-\lambda_{210Po}(t_{plat1}-t_{extr})} \right) e^{\lambda_{210Po}(t_{plat1}-t_{extr})}$$

$$- \frac{\lambda_{210Po}(A_{210Pb})_B}{\lambda_{210Po} - \lambda_{210Pb}} \left(e^{-\lambda_{210Pb}(t_{extr}-t_{car})} - e^{-\lambda_{210Po}(t_{extr}-t_{car})} \right) e^{\lambda_{210Po}(t_{extr}-t_{car})}$$

Eq. 12b

$$\sigma((A_{210Po})_B) = \sqrt{\begin{aligned} & \sigma\left((A_{210Po})_{sol,t_{plat1}}\right)^2 \left(e^{\lambda_{210Po}(t_{plat1}-t_{car})}\right)^2 \\ & + \sigma((A_{210Pb})_B)^2 \left(\frac{\lambda_{210Po} e^{-\lambda_{210Pb}(t_{extr}-t_{car})} f_{Pb_{rec1}}}{\lambda_{210Po} - \lambda_{210Pb}} \left(e^{-\lambda_{210Pb}(t_{plat1}-t_{extr})} - e^{-\lambda_{210Po}(t_{plat1}-t_{extr})}\right) e^{\lambda_{210Po}(t_{plat1}-t_{extr})}\right)^2 \\ & + \sigma((A_{210Pb})_B)^2 \left(\frac{\lambda_{210Po}}{\lambda_{210Po} - \lambda_{210Pb}} \left(e^{-\lambda_{210Pb}(t_{extr}-t_{car})} - e^{-\lambda_{210Po}(t_{extr}-t_{car})}\right) e^{\lambda_{210Po}(t_{extr}-t_{car})}\right)^2 \\ & + \sigma(f_{Pb_{rec1}})^2 \left(\frac{\lambda_{210Po} (A_{210Pb})_B e^{-\lambda_{210Pb}(t_{extr}-t_{car})}}{\lambda_{210Po} - \lambda_{210Pb}} \left(e^{-\lambda_{210Pb}(t_{plat1}-t_{extr})} - e^{-\lambda_{210Po}(t_{plat1}-t_{extr})}\right) e^{\lambda_{210Po}(t_{plat1}-t_{extr})}\right)^2 \end{aligned}}$$

Eq. 13a

$$(A_{210Po})_{spl,t_{spl}} \left(\frac{dpm}{100kg}\right) = \frac{(A_{210Po})_{spl,t_{spl}}}{m_{spl}} 100$$

Eq. 13b

$$\sigma\left((A_{210Po})_{spl,t_{spl}} \left(\frac{dpm}{100kg}\right)\right) = \sqrt{\sigma\left((A_{210Po})_{spl,t_{spl}}\right)^2 \left(\frac{100}{m_{spl}}\right)^2}$$

Eq. 14b

[illegible]